ASM Handbook, Volume 22A: Fundamentals of Modeling for Metals Processing
D.U. Furrer and S.L. Semiatin, editors, p 203-219

Modeling of Nucleation Processes

Emmanuel Clouet, CEA, DEN, Service de Recherches de Métallurgie Physique, France

NUCLEATION is the onset of a first-order phase transition by which a metastable phase transforms into a more stable one. Such a phase transition occurs when a system initially in equilibrium is destabilized by the change of an external parameter such as temperature or pressure. If the perturbation is small enough, the system does not become unstable but rather stays metastable. In diffusive transformations, the system then evolves through nucleation, the growth and coarsening of a second phase. Such a phase transformation is found in many situations in materials science, such as condensation of liquid droplets from a supersaturated vapor, solidification, precipitation from a supersaturated solid solution, and so on. The initial stage of all these different processes can be well described within the same framework, currently known as the classical nucleation theory.

Since its initial formulation in 1927 by Volmer, Weber, and Farkas (Ref 1, 2) and its modification in 1935 by Becker and Döring (Ref 3), the classical nucleation theory has been a suitable tool to model the nucleation stage in phase transformations. The success of this theory relies on its simplicity and on the few parameters required to predict the nucleation rate, that is, the number of clusters of the new phase appearing per unit of time and volume. It allows rationalizing experimental measurements, predicting the consequences of a change of the control parameters such as temperature or supersaturation, and describing the nucleation stage in mesoscopic modeling of phase transformations.

This article first describes the results obtained by Volmer, Weber, Farkas, Becker, and Döring (Ref 1–3), which constitute the classical nucleation theory. These results are the predictions of the precipitate size distribution, steady-state nucleation rate, and incubation time. This theory describes the nucleating system as a homogeneous phase where heterophase fluctuations occur. Some of these fluctuations reach a large enough size that they can continue to grow and lead to the formation of precipitates. The nucleating system is thus envisioned mainly from a thermodynamic viewpoint. The key controlling parameters are the nucleation driving force and the interface free energy. A kinetic approach, cluster dynamics, can also be used to describe nucleation. This constitutes the second part of this article. Here, a master equation describes the time evolution of the system, which is modeled as a cluster gas. The key parameters are the cluster condensation and evaporation rates. Both approaches are different in their description of the nucleating system and their needed input parameters. They are nevertheless closely related. Predictions of the classical nucleation theory have actually been derived from the same master equation used by cluster dynamics (Ref 3), and extensions of classical nucleation theory always start from this master equation. In this article, the links as well as the difference between both descriptions are emphasized. Since its initial formulation, the classical nucleation theory has been enriched, mainly by Binder and Stauffer (Ref 4–6), to take into account the fact that clusters other than monomers can migrate and react. It has also been extended to multicomponent systems (Ref 7–12). These generalizations of the initial formalism are presented at the end of the second part.

Thermodynamic Approach

Conditions for Nucleation

Nucleation occurs when a homogeneous phase initially in stable thermal equilibrium is put in a state where it becomes metastable by the variation of a controlling parameter. In the following case, the controlling parameter is the temperature, and the initial system is quenched through a first-order phase transition in a two-phase region. The system then tends to evolve toward a more stable state and to reach its equilibrium. Because the parent phase is not unstable, this transformation cannot proceed through the continuous development of growing infinitesimal perturbations delocalized in the whole phase, that is, by spinodal decomposition (Ref 13, 14). Such perturbations in a metastable state increase the free energy. As a consequence, they can appear because of thermal fluctuations, but they naturally decay. To reach its equilibrium, the system must overcome an energy barrier to directly form clusters of the new equilibrium phase, a process known as nucleation.

This difference between a metastable and an unstable state, as well as between nucleation and spinodal decomposition, is better understood through the following example. Consider a system corresponding to a binary mixture of two elements, A and B, with a fixed atomic fraction x of B elements. Such a system can be a solid or a liquid solution, for instance. Assume that the free energy per atom, $G(x)$, of this system is known for every composition x and is given by the function plotted in Fig. 1. A two-phase region given by the common tangent construction exists at the considered temperature; the equilibrium state of binary mixtures with an intermediate composition x^0 between x^e and y^e corresponds to a mixture of two phases having the compositions x^e and y^e. A homogeneous system with a composition x^0 will then separate into these two equilibrium phases. The variation of the free energy can be examined if this transformation happens through the development of infinitesimal fluctuations. In that purpose, consider a small perturbation corresponding to a separation of the initially homogeneous system into two phases having the compositions $x^0 + \mathrm{d}x_1$ and $x^0 + \mathrm{d}x_2$. For the perturbation to be small, assume $|\mathrm{d}x_1| \ll 1$ and $|\mathrm{d}x_2| \ll 1$. If f_1 is the fraction of phase 1, matter conservation imposes the following relation between both compositions:

$$f_1 \mathrm{d}x_1 + (1 - f_1)\mathrm{d}x_2 = 0 \qquad \text{(Eq 1)}$$

The free energy variation associated with this unmixing is given by:

$$\begin{aligned}\Delta G &= f_1 G\left(x^0 + \mathrm{d}x_1\right) + (1 - f_1) G\left(x^0 + \mathrm{d}x_2\right) \\ &\quad - G\left(x^0\right) \\ &= \tfrac{1}{2}\left[f_1 \mathrm{d}x_1^2 + (1 - f_1)\mathrm{d}x_2^2\right] G''(x^0) + \mathrm{o}\left(\mathrm{d}x_1^2\right)\end{aligned} \qquad \text{(Eq 2)}$$

The first derivative $G'(x^0)$ of the free energy does not appear in Eq 2 because of the relation in Eq 1. The sign of the free-energy variation is

thus governed by the second derivative $G''(x^0)$ of the free energy. If this second derivative is negative, the initial infinitesimal perturbation decreases the free energy (Fig. 2a). It can therefore develop until the system reaches its two-phase equilibrium state. This is the regime of spinodal decomposition. In Fig. 1, the free-energy second derivative changes its signs in x^s and y^s; all homogeneous systems with a composition between these limits are unstable and evolve spontaneously to equilibrium. On the other hand, if the composition x^0 is higher than the equilibrium composition x^e but smaller than the spinodal limit x^s, the homogeneous binary mixture is metastable. Because the second derivative of the free energy is positive, any infinitesimal perturbation increases the free energy (Fig. 2b) and will therefore decay. To reach its equilibrium state, the system must overcome an energy barrier, and phase separation occurs by nucleation of the new equilibrium phase with the composition y^e.

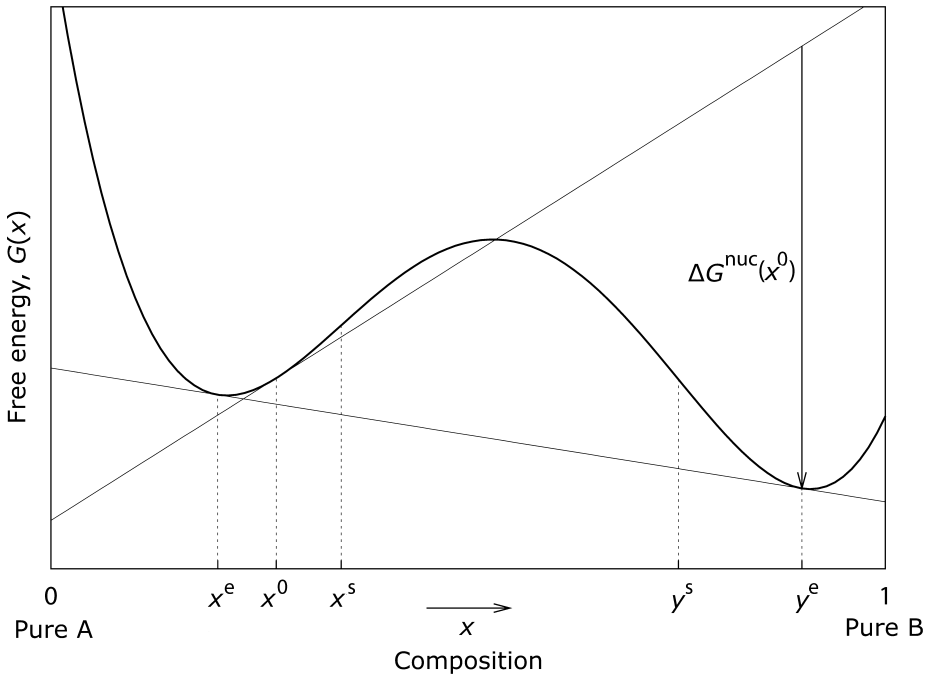

Fig. 1 Sketch of the free energy of a binary mixture quenched in a two-phase region. The bold line is the free energy per atom $G(x)$ of the homogeneous system. The compositions x^e and y^e of the equilibrium phases are given by the common tangent construction. The spinodal limits x^s and y^s define the unstable region. $\Delta G^{nuc}(x^0)$ is the nucleation free energy of the metastable homogeneous system of composition x^0.

The Capillary Approximation

In the nucleation regime, the system evolves through the formation of well-defined and localized fluctuations corresponding to clusters of the new equilibrium phase. The formation free energies of these clusters are well described by the capillary approximation. This assumes that two contributions enter this free energy (Fig. 3):

- *Volume contribution*: By forming a cluster of the new phase, the system decreases its free energy. The gain is directly proportional to the volume of the cluster or, equivalently, to the number, n, of atoms forming the cluster. This is the nucleation driving force.
- *Surface contribution*: One needs to create an interface between the parent phase and the cluster of the new phase. This interface has a cost that is proportional to the surface area of the cluster or, equivalently, to $n^{(d-1)/d}$, where d is the dimension of the system.

The following is restricted to the three-dimensional case. The formation free energy of a cluster containing n atoms is then given by:

$$\Delta G_n = n\Delta G^{nuc} + n^{2/3} A\sigma \qquad \text{(Eq 3)}$$

where ΔG^{nuc} is the nucleation free energy, σ is the interface free energy, and A is a geometric factor. If the interface free energy is isotropic, the equilibrium shape of the cluster is a sphere. The corresponding geometric factor is then $A = (36\pi\Omega_1^2)^{1/3}$, where Ω_1 is the volume of a monomer. For anisotropic interface free energy, one can use the Wulff construction (Ref 15, 16) to determine the equilibrium shape, that is, the shape with minimum free energy for a given volume, and deduce an average interface free energy corresponding to a hypothetical spherical cluster having the same volume and the same interface energy as the real one, which may be facetted. An example is given in Ref 17 for precipitates with {100}, {110}, and {111} interfaces.

The nucleation free energy is obtained by considering the difference of chemical potentials in the parent and in the equilibrium phases for all atoms composing the cluster:

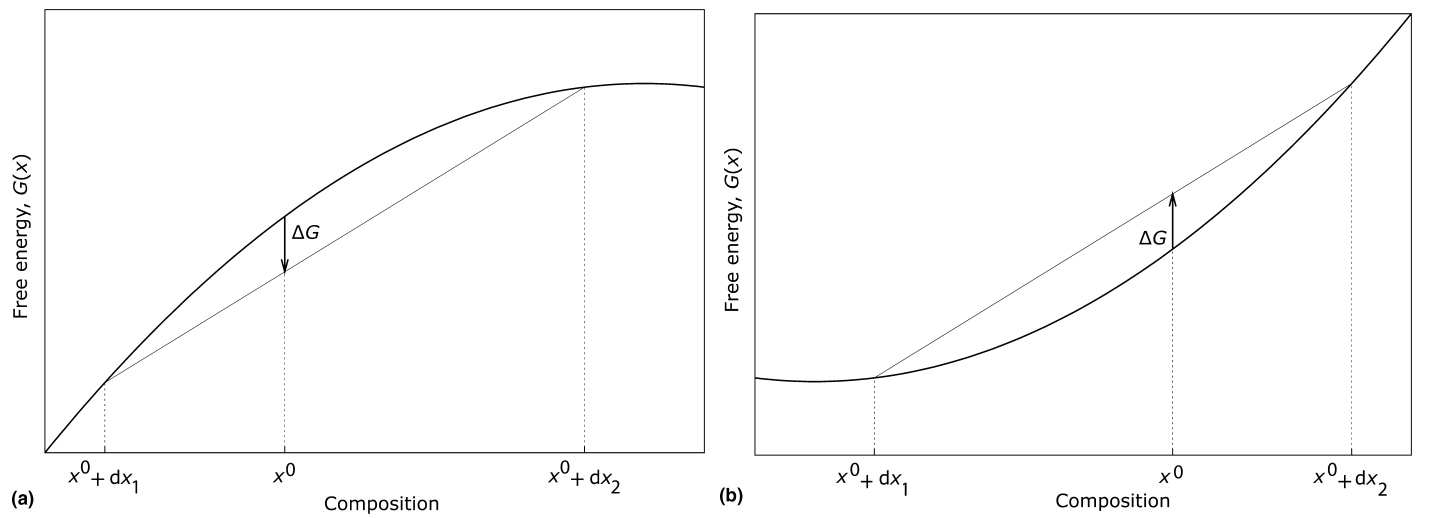

Fig. 2 Variation ΔG of the free energy corresponding to the spontaneous unmixing of a homogeneous system of composition x^0 in two phases of respective compositions $x^0 + dx_1$ and $x^0 + dx_2$. (a) Spinodal regime ($G''(x^0) < 0$). (b) Nucleation regime ($G''(x^0) > 0$)

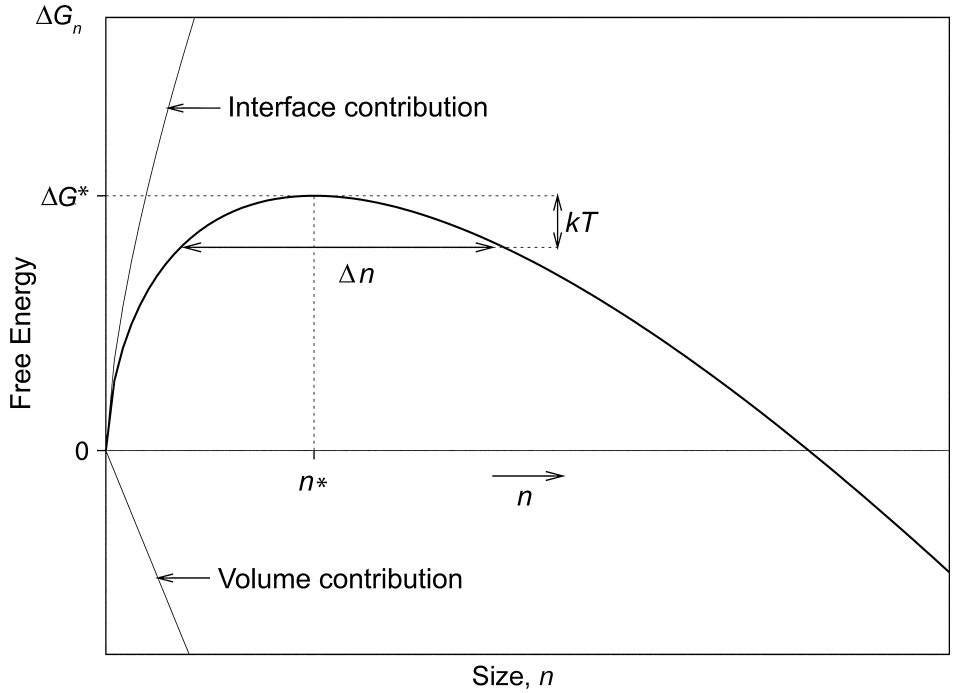

Fig. 3 Variation of the cluster formation free energy ΔG_n with the number, n, of atoms they contain as described by Eq 3. n^* is the critical size and ΔG^* the corresponding free energy. The size interval Δn characterizes the energy profile around the critical size and is directly linked to the Zeldovich factor (Eq 10).

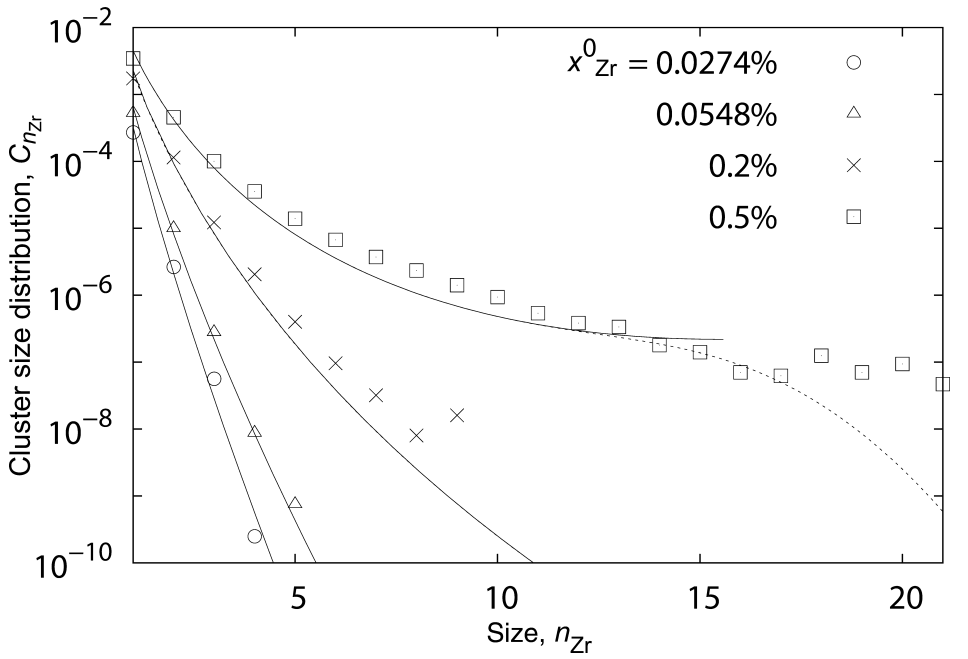

Fig. 4 Dependence on the nominal concentration x^0_{Zr} of the cluster size distribution of an aluminum solid solution at 500 °C. At this temperature, the solubility limit is $x^e_{Zr} = 0.0548$ %. Symbols correspond to atomic simulations (kinetic Monte Carlo) (Ref 18) and lines to predictions of the classical nucleation theory. Full lines correspond to the equilibrium cluster size distribution (Eq 7) for $n \leq n^*$ and dotted lines to the steady-state distributions (Eqs 8 and 85).

$$\Delta G^{\text{nuc}} = \sum_i y_i^e(\mu_i^e - \mu_i^0) \quad \text{(Eq 4)}$$

where y_i^e is the atomic fraction of the type i atom in the nucleating equilibrium phase, and μ_i^e and μ_i^0 are the corresponding chemical potentials in the nucleating equilibrium phase and the parent phase, respectively. When the parent phase is metastable, chemical potentials in this phase are higher than the ones at equilibrium. The nucleation free energy given by Eq 4 is therefore negative. Classic expressions of the nucleation free energy are given at the end of this section in some simple cases. For negative nucleation driving force, because of the competition between the volume and the interface contributions, the cluster formation free energy (Eq 3) shows a maximum for a given critical size, n^*, as illustrated in Fig. 3. n^* corresponds to the size at which the first derivative of ΔG_n is equal to zero, thus leading to:

$$n^* = \left(-\tfrac{2}{3}\frac{A\sigma}{\Delta G^{\text{nuc}}}\right)^3 \quad \text{(Eq 5)}$$

and the corresponding formation free energy:

$$\Delta G^* = \Delta G_{n^*} = \tfrac{4}{27}\frac{(A\sigma)^3}{(\Delta G^{\text{nuc}})^2} \quad \text{(Eq 6)}$$

Below this critical size, the energy of growing clusters increases because of the interface predominance at small sizes. Clusters in this size range are therefore unstable; if a cluster is formed, it will tend to redissolve. Nevertheless, unstable clusters can be found in the parent phase because of thermal fluctuations. The size distribution of these clusters is given by:

$$C_n^{\text{eq}} = C_0 \exp\left(-\frac{\Delta G_n}{kT}\right) \quad \text{(Eq 7)}$$

where C_0 is the atomic fraction of sites accessible to the clusters. For precipitation in the solid state, for instance, all lattice sites can receive a cluster, and therefore $C_0 = 1$. The validity of the size distribution (Eq 7) can be demonstrated for an undersaturated system ($\Delta G^{\text{nuc}} \geq 0$) using a lattice gas model (compare with "Cluster Gas Thermodynamics" in the "Kinetic Approach" section of this article). For a supersaturated system, one assumes that the system reaches a steady state where clusters smaller than the critical size still obey the distribution (Eq 7).

Comparisons with atomic simulations have shown that Eq 7 correctly describes the size distribution of subcritical clusters. An example of such a comparison is given in Fig. 4 for aluminum-zirconium alloys, leading to the coherent precipitation of $L1_2$ Al_3Zr compounds (Ref 17); size distributions are given for undersaturated, saturated, and supersaturated solid solutions. A similar comparison leading to the same conclusion can be found in Ref 18 for an unmixing alloy on a body-centered cubic lattice, or in Ref 19 and 20 for the magnetization reversal of an Ising model in two and three dimensions, respectively.

The kinetic approach developed further in this article shows that the steady-state distribution in a nucleating system slightly deviates from the equilibrium distribution (Eq 7) around the critical size. An exact expression of the steady-state distribution has been obtained by Kashiev (Ref 21, 22). In the critical size interval, Δn, which is precisely defined as follows, it can be approximated by:

$$C_n^{\text{st}} = [\tfrac{1}{2} - Z(n - n^*)]C_n^{\text{eq}} \quad \text{(Eq 8)}$$

The Zeldovich factor, Z, appearing in this equation is a function of the second derivative

of the cluster formation free energy at the critical size:

$$Z = \sqrt{-\frac{1}{2\pi kT}\frac{\partial^2 \Delta G_n}{\partial n^2}\bigg|_{n=n^*}} = \frac{3(\Delta G^{\text{nuc}})^2}{4\sqrt{\pi kT}(A\sigma)^{3/2}} \quad \text{(Eq 9)}$$

The physical meaning of the Zeldovich factor can be seen in Fig. 3, which sketches the variation of the cluster formation free energy with their size. If the formation free energy was harmonic, the size interval where the difference between the cluster free energy and the nucleation barrier, ΔG^*, is smaller than the thermal energy, kT, would be given by:

$$\Delta n = \frac{2}{\sqrt{\pi}}\frac{1}{Z} \quad \text{(Eq 10)}$$

The Zeldovich factor therefore characterizes the flatness of the energy profile around the critical size. Equation 8 shows that steady-state cluster concentrations in the critical region are reduced compared to the equilibrium distribution. For the critical size, a factor ½ appears in front of the equilibrium concentration.

Steady-State Nucleation Rate

When the nucleation barrier, ΔG^*, is high enough compared to the thermal energy, kT, the metastable state of the system contains thermal fluctuations well described by the distribution (Eq 7). Sometimes, one of these fluctuations will reach and overcome the critical size. It can then continue to grow and become more and more stable. Classical nucleation theory assumes that the system reaches a steady state, and it then shows that stable nuclei appear at a rate given by (Ref 3):

$$J^{\text{st}} = \beta^* Z C_0 \exp\left(-\frac{\Delta G^*}{kT}\right) \quad \text{(Eq 11)}$$

where β^* is the rate at which a critical cluster grows, and Z is the Zeldovich factor (Eq 9). This factor has been introduced by Becker and Döring (Ref 3) to describe cluster fluctuations around the critical size and, in particular, the probability for a stable nucleus to redissolve. $ZC_0 \exp(-\Delta G^*/kT)$ is therefore the number of critical clusters that reach a size large enough that they can continuously grow. The initial expression of the nucleation rate derived by Volmer and Weber (Ref 1) and by Farkas (Ref 2) did not consider this Zeldovich factor and led to an overestimation of the nucleation rate. A small Zeldovich factor corresponds to a flat energy profile around the critical size. Critical clusters experience size variations that are mainly random and not really driven by their decrease in energy. Some of them will redissolve and not fall in the stable region. This explains why the nucleation rate is reduced by the Zeldovich factor. A more rigorous derivation of the nucleation rate where the Zeldovich factor naturally appears is given in the section "The Link with Classical Nucleation Theory" in this article.

An expression for the growing rate β^* of the critical cluster is needed. If the growth-limiting process is the reaction at the interface to attach the atoms on the critical cluster (ballistic regime), β^* is then proportional to the cluster area. Assuming that this reaction is controlled by one type of atom, the following expression is obtained (Ref 23):

$$\beta^* = 4\pi r^{*2}\frac{\lambda_i \Gamma_i}{\Omega}\frac{x_i^0}{y_i^e} \quad \text{(Eq 12)}$$

where r^* is the radius of the critical cluster, λ_i is the distance corresponding to the atom last jump to become attached to the critical cluster, Γ_i is the corresponding reaction frequency, and Ω is the volume corresponding to one atomic site. x_i^0 and y_i^e are the respective atomic fraction of the jumping atoms in the metastable parent phase and the stable nucleating phase.

For solid - solid phase transformations, the critical cluster growth is usually controlled by the long-range diffusion of solute atoms. The critical condensation rate is then obtained by solving the classical diffusion problem associated with a growing spherical particle. If diffusion of only one type of atom limits the growth, and all other atomic species diffuse sufficiently fast enough so that the cluster composition instantaneously adjusts itself, one obtains (Ref 23):

$$\beta^* = 4\pi r^*\frac{D_i}{\Omega}\frac{x_i^0}{y_i^e} \quad \text{(Eq 13)}$$

where D_i is the diffusion coefficient of type i atoms. In a multicomponent alloy, when diffusion coefficients of different atomic species have close values and when the composition of the critical cluster can vary, one must use the linked flux analysis presented in the section "Cluster Dynamics" in this article. In all cases, the growth rate is proportional to the cluster radius in this diffusive regime.

Both events, that is, the long-range diffusion and the reaction at the interface, can be simultaneously taken into account. The corresponding expression of the condensation rate has been derived by Waite (Ref 24).

Transient Nucleation

A transient regime exists before the nucleation rate reaches its stationary value (Eq 11). One conventionally defines an incubation time, or a time lag, to characterize this transient regime. This is defined as the intercept with the time axis of the tangent to the curve representing the variations of the nuclei density (Fig. 5). Exact expressions of the incubation time have been obtained as a series of the initial and steady-state cluster size distributions (Ref 26, 27). Different approximations have then been made to evaluate this series and obtain closed forms of the incubation time. They all lead to an incubation time:

$$t_{\text{inc}}(n^*) = \theta_0\frac{1}{\pi Z^2 \beta^*} = \theta_0\frac{16kT(A\sigma)^3}{9(\Delta G^{\text{nuc}})^4 \beta^*} \quad \text{(Eq 14)}$$

where the factor θ_0 depends on the chosen approximation and is close to 1 (Ref 28). Some authors obtained a factor θ_0 that depends slightly on the temperature and the shape of the

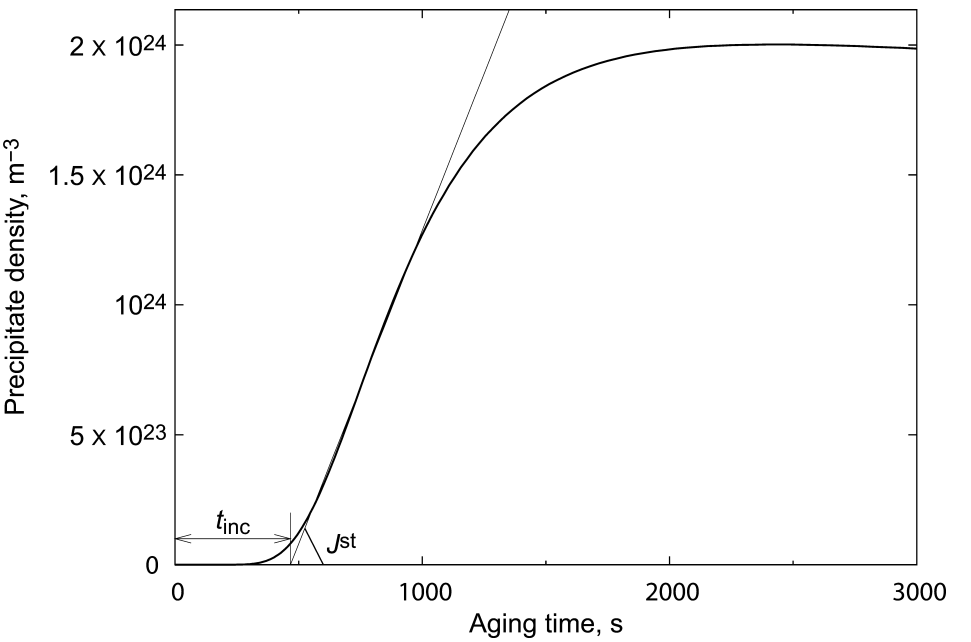

Fig. 5 Precipitate density as a function of aging time for an aluminum solid solution containing 0.18 at.% Sc aged at 300 °C. The time evolution obtained from cluster dynamics simulations (Ref 25) allows the definition of a steady-state nucleation rate, J^{st}, and an incubation time, t_{inc}.

cluster formation free energy around the critical size (Ref 26, 29). One can stress, however, that a precise value of this factor is seldom, if ever, needed. As is shown later, the incubation time depends on too many parameters to be known precisely experimentally. Equation 14 allows describing its main variation when the temperature or the nucleation driving force are changed; this is usually enough to model incubation and nucleation.

This expression (Eq 14) of the incubation time can be obtained from simple physical considerations (Ref 23, 30). The steady state will be reached once the clusters have grown sufficiently far away from the critical size. Supercritical clusters have a negligible probability to decay when their size becomes greater than $n^* + \frac{1}{2}\Delta n$. Δn characterizes the width of the critical region (Fig. 3) and is related to the Zeldovich factor via Eq 10. Because the energy profile is flat in this neighborhood, clusters make a random walk in the size space, with a constant jump frequency β^*. Accordingly, the corresponding time needed to diffuse from n^* to $n^* + \frac{1}{2}\Delta n$ is:

$$t_{\text{inc}}(n^*) \sim \frac{\Delta n^2}{4\beta^*} \qquad \text{(Eq 15)}$$

This leads to the expression (Eq 14) with a factor $\theta_0 = 1$.

Different approximations of the nucleation rate in this transient regime can also be found in the literature. Kelton et al. (Ref 28) have compared these approximations with exact results obtained, thanks to a numerical integration of the kinetic equations describing nucleation. They concluded that the best-suited approximation to describe the transient nucleation rate is the one obtained by Kashchiev (Ref 21, 22):

$$J(t) = J^{\text{st}}\left[1 + 2C\sum_{m=1}^{\infty}(-1)^m \exp\left(-\frac{m^2 t}{\tau}\right)\right] \qquad \text{(Eq 16)}$$

where $C = 1$ for a system initially prepared in a state far from its nucleating metastable state. The time constant is given by:

$$\tau = \frac{4}{\pi^3}\frac{1}{Z^2\beta^*} \qquad \text{(Eq 17)}$$

When $t > \tau$, one can retain only the first term in the sum appearing in Eq 16. Usually, it is even enough to assume that the nucleation rate behaves like the Heaviside step function; that is, that the nucleation rate reaches its stationary value after an incubation time where no nucleation occurs. The incubation time corresponding to Eq 16 is $\pi^2\tau/6$. Therefore, in the Kashchiev treatment, the factor in Eq 14 is $\theta_0 = \frac{2}{3}$.

It is worth saying that the incubation time and the associated transient regime depend on the conditions in which the system has been prepared. Equations 14 and 16 implicitly assume that the quench was done from infinite temperature; no cluster around the critical one existed at the initial time. This may not be true. For instance, the system could have been prepared in an equilibrium state corresponding to a slightly higher temperature where it was stable and then quenched in a metastable state. A cluster distribution corresponding to this higher temperature already exists before the beginning of the phase transformation. If the temperature difference of the quench is small, these preexisting clusters will reduce the incubation period. The dependence of the incubation time on the initial conditions has been observed, for instance, in atomic simulations for an unmixing binary alloy (Ref 18). Starting from a random solid solution corresponding to an infinite temperature preparation, an incubation time is observed before nucleation reaches its steady state. If the alloy is annealed above its solubility limit before a quench, the incubation stage disappears if the temperature difference of the quench is not too high. Kashchiev considered the effect of this initial cluster distribution on nucleation in the case of a change in pressure (Ref 22, 31). His results can be easily generalized (Ref 28). To do so, the supersaturation variation is introduced:

$$\Delta s = \frac{\Delta G^{\text{nuc}}(t = 0^-)}{kT(t = 0^-)} - \frac{\Delta G^{\text{nuc}}(t = 0^+)}{kT(t = 0^+)} \qquad \text{(Eq 18)}$$

where $t = 0^-$ means that thermodynamic quantities are calculated for the initial state in which the system has been prepared, and $t = 0^+$ for the state where nucleation occurs. In his derivation, Kashchiev assumed that the interface free energy of the clusters is the same in both stable and metastable states. The constant entering in the expression (Eq 16) of the transient nucleation rate is then:

$$C = 1 - \frac{\Delta s}{Z}\exp(-n^*\Delta s) \qquad \text{(Eq 19)}$$

and the corresponding incubation time is multiplied by this constant C. The supersaturation variation, Δs, is positive; otherwise, nucleation would have happened in the initial state in which the system has been prepared. The existence of an initial cluster size distribution therefore always reduces the incubation time. Nevertheless, C rapidly tends to 1 when the thermodynamic states $t = 0^-$ and $t = 0^+$ become too different.

By definition, the nucleation rate does not depend on the cluster size in the stationary regime. This property is used to advantage in Eq 11 to calculate the steady-state nucleation rate, J^{st}, at the critical size. However, the time needed for the stationary regime to develop will, of course, vary with the cluster size. This means that the incubation time depends on the cluster size at which it is measured. The previously defined incubation time corresponds to the critical size. However, the smallest cluster size that one can detect experimentally may be significantly larger than the critical size. Therefore, it is necessary to describe the variation with the cluster size of the incubation time. This problem has been solved by Wu (Ref 26) and Shneidman and Weinberg (Ref 29), who showed that the incubation time measured at size n is:

$$t_{\text{inc}}(n) = t_{\text{inc}}(n^*) + \frac{1}{2\pi Z^2\beta^*}\left\{\theta_1 + \ln\left[\sqrt{\pi}Z(n - n^*)\right]\right\} \qquad \text{(Eq 20)}$$

for $n > n^* + \Delta n$, that is, a cluster size outside the critical region. The constant θ_1 is 1 in the expression obtained by Wu and $\theta_1 = \gamma/4 + \ln(2)/2$ for Shneidman and Weinberg, where $\gamma \sim 0.5772$ is Euler's constant.

All the aforementioned expressions are obtained in the parabolic approximation, that is, assuming that the cluster formation free energy is well described by its harmonic expansion around the critical size. According to Shneidman and Weinberg (Ref 29), this approximation is highly accurate when calculating the steady-state nucleation rate, but its validity is limited for the incubation time. When considering the exact shape of the cluster formation free energy (Eq 3), the expression of the incubation time then depends on the model used for the absorption rate. In all cases, the incubation time at the critical size can be written:

$$t_{\text{inc}}(n^*) = \frac{1}{2\pi Z^2\beta^*}\left[\frac{\gamma}{2} + \ln\left(\sqrt{\pi}Zn^*\right) - \theta_3\right] \qquad \text{(Eq 21)}$$

where the constant θ_3 differs from 0 when the parabolic approximation is not used. In the ballistic regime, when the condensation rate is proportional to the cluster surface, such as in Eq 12, the authors obtained $\theta_3 = 1 - \ln(3)$. The incubation time measured at size n is then:

$$t_{\text{inc}}(n) = \frac{1}{2\pi Z^2\beta^*}\left\{\left(\frac{n}{n^*}\right)^{1/3} + \ln\left[\left(\frac{n}{n^*}\right)^{1/3} - 1\right] + \gamma - 2 + \ln\left[\frac{6\Delta G^*}{kT}\right]\right\}, \quad \forall n > n^* + \tfrac{1}{2}\Delta n \qquad \text{(Eq 22)}$$

In the diffusive regime, when the condensation rate is proportional to the cluster radius, such as in Eq 13, $\theta_3 = 3/2 - \ln(3)$ and:

$$t_{\text{inc}}(n) = \frac{1}{2\pi Z^2\beta^*}\left\{\tfrac{1}{2}\left[\left(\tfrac{n}{n^*}\right)^{1/3} + 2\right]^2 + \ln\left[\left(\tfrac{n}{n^*}\right)^{1/3} - 1\right] + \gamma - \tfrac{7}{2} + \ln\left[\tfrac{6\Delta G^*}{kT}\right]\right\}, \quad \forall n > n^* + \tfrac{1}{2}\Delta n. \qquad \text{(Eq 23)}$$

It should be stressed that all these expressions for incubation time have been obtained in the continuous limit valid for large clusters. The expressions should be used only when the nucleation barrier ΔG^* is high enough for the critical size not being too small.

Heterogeneous Nucleation

Until now, only homogeneous nucleation has been considered; it was assumed that nuclei can form anywhere in the system. However, it may

require less energy for the nuclei to form heterogeneously on preferred nucleation sites. These sites can be at the interface with existing impurities or some lattice defects such as grain boundaries or dislocations. The classical theory also allows modeling heterogeneous nucleation after some slight modifications. The first modification is that the parameter C_0 appearing in the cluster size distribution (Eq 7) is now the number of sites where heterogeneous precipitation can take place. One also needs to take into account the decrease of the nuclei free energy when they are located at a preferred nucleation site. Such a decrease usually arises from a gain in the interface free energy; it is more favorable for the nuclei to form on an already existing interface, because the cost to create the interface between the old and the new phases is reduced.

First consider the case where the cluster wets the substrate and has a cap shape (Fig. 6a). Electrodeposition is one example where this happens (Ref 32). Three different interface free energies must be considered:

- σ between the parent and the nucleating phase
- σ_s between the parent phase and the substrate
- σ_i between the nucleating phase and the substrate

The wetting angle is then defined by the Young equilibrium equation (Ref 16):

$$\cos\theta_w = \frac{\sigma_s - \sigma_i}{\sigma} \qquad \text{(Eq 24)}$$

The wetting leads to a cap shape only if the interface free energies obey the inequalities $-\sigma \le \sigma_s - \sigma_i \le \sigma$. If the difference $\sigma_s - \sigma_i$ is smaller than $-\sigma$, then $\theta_w = \pi$, and the wetting is not possible because an unwet cluster costs less energy. On the other hand, if the difference is greater than σ, the wetting is complete, and one can no longer define a cap shape because the nucleating phase will uniformly cover the interface.

The cluster free energy takes the same expression as the one given by the capillary approximation in the homogeneous case (Eq 3). To calculate the geometric factor A appearing in this expression, the radius, R, of the cap must be defined. The cluster volume is then given by (Ref 22):

$$n\Omega_1 = \tfrac{1}{3}\pi R^3(2+\cos\theta_w)(1-\cos\theta_w)^2 = \pi R^3\frac{(2\sigma+\sigma_s-\sigma_i)(\sigma-\sigma_s+\sigma_i)^2}{3\sigma^3} \qquad \text{(Eq 25)}$$

and the free energy associated with the whole cluster interface by:

$$n^{2/3}A\sigma = \pi R^2\left[\sigma 2(1-\cos\theta_w) + (\sigma_i-\sigma_s)\sin^2\theta_w\right] = \pi R^2(\sigma-\sigma_s+\sigma_i) \times \frac{2\sigma^2+(\sigma_i-\sigma_s)(\sigma+\sigma_s-\sigma_i)}{\sigma^2} \qquad \text{(Eq 26)}$$

Eliminating the variable R between Eq 25 and 26, one obtains the expression of the geometric factor appearing in the capillary approximation:

$$A = \left(9\pi\Omega_1^2\right)^{1/3}\frac{2\sigma^2-(\sigma_s-\sigma_i)(\sigma+\sigma_s-\sigma_i)}{\sigma(2\sigma+\sigma_s-\sigma_i)^{2/3}(\sigma-\sigma_s+\sigma_i)^{1/3}} \qquad \text{(Eq 27)}$$

When $\sigma_s - \sigma_i = \sigma$, the unwetting is complete; one recovers the geometric factor $A = \left(36\pi\Omega_1^2\right)^{1/3}$ corresponding to a spherical cluster. With this expression of the geometric factor and the correct value of the parameter C_0, all expressions obtained for homogeneous nucleation can also be used for heterogeneous nucleation.

Nuclei can also have a lens shape (Fig. 6b). In such a case, the two wetting angles are defined by (Ref 22):

$$\cos\theta_w = \left(\sigma_s^2+\sigma^2-\sigma_i^2\right)/2\sigma_s\sigma \qquad \cos\theta_s = \left(\sigma_s^2+\sigma^2-\sigma_i^2\right)/2\sigma_s\sigma_i \qquad \text{(Eq 28)}$$

The geometric factor corresponding to this lens shape is obtained using the same method as previously; one expresses the volume and the interface energy of the two caps composing the cluster and then eliminates the cap radii between these two equations.

Examples

It is worth having a closer look at some examples—solidification and precipitation in the solid state—and giving an approximated expression of the nucleation free energy in these simple cases.

Example 1: Solidification. A single component liquid that was initially at equilibrium is quenched at a temperature, T, below its melting temperature, T_m. Because the liquid and the solid have the same composition, the nucleation free energy is simply the free-energy difference between the liquid and the solid states at the temperature T. If the undercooling is small, one can ignore the difference in the specific heats of the liquid and the solid. The nucleation free energy is then proportional to the latent heat of fusion per atom, L (Ref 16):

$$\Delta G^{nuc} = L\frac{T-T_m}{T_m} \qquad \text{(Eq 29)}$$

When the undercooling is large, Eq 29 may be not precise enough. One can then consider the next term in the Taylor expansion (Ref 22), leading to:

$$\Delta G^{nuc} = L\frac{T-T_m}{T_m} - \Delta C_p\frac{(T-T_m)^2}{2T_m} \qquad \text{(Eq 30)}$$

where $\Delta C_p = C_p^{liq}(T_m) - C_p^{sol}(T_m)$ is the difference in the heat capacities of the liquid and solid phases.

Equation 29 shows how the steady-state nucleation rate varies with the quenching temperature. Assuming that the interface free energy is constant and that the condensation rate, β^*, simply obeys an Arrhenius law, one obtains the nucleation rate given by:

$$J^{st} = \lambda\frac{(T-T_m)^2}{\sqrt{T}}\exp\left[-\left(\frac{A}{T}+\frac{B}{T(T-T_m)^2}\right)\right] \qquad \text{(Eq 31)}$$

where λ, A, and B are positive constants. The nucleation rate corresponding to this equation is sketched in Fig. 7. The main variations are given by the exponential. As a consequence, there is a temperature window in which the nucleation rate is substantial. For high temperatures close to the melting temperature, T_m, the nucleation free energy is small and leads to a negligible nucleation rate. At low temperatures, the nucleation rate is also negligible because of the Arrhenian behavior of the kinetic factor and the critical cluster concentration (Eq 7). The nucleation rate can be measured only at intermediate

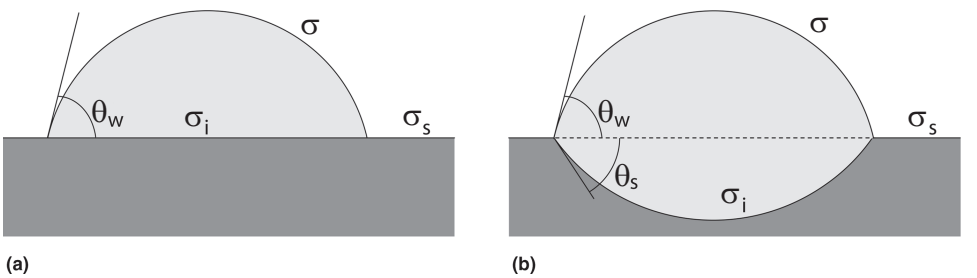

Fig. 6 Possible shapes of a nucleus in heterogeneous nucleation. (a) Cap shape. (b) Lens shape

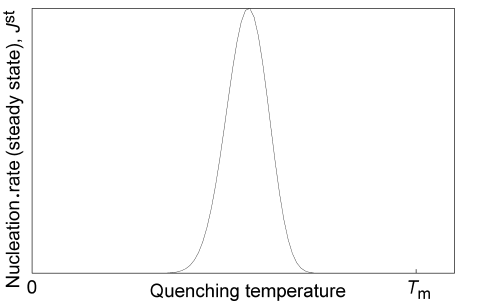

Fig. 7 Variation with quenching temperature of steady-state nucleation rate in the case of solidification (Eq 31). T_m, melting temperature

temperatures. Such conclusions on the nucleation rate are not specific to solidification but are encountered in any nucleation experiment.

Example 2: Precipitation in the Solid State. In this example, it is necessary to take into account elastic effects. The free energy is thus divided between a chemical and an elastic contribution.

Chemical Contribution. For the binary mixture, whose free energy per atom $G(x)$ is sketched in Fig. 1, the homogeneous metastable phase of composition x^0 has a nucleation free energy given by:

$$\Delta G^{\text{nuc}}(x^0) = (1-y^{\text{e}})\left[\mu_{\text{A}}(y^{\text{e}}) - \mu_{\text{A}}(x^0)\right] + y^{\text{e}}\left[\mu_{\text{B}}(y^{\text{e}}) - \mu_{\text{B}}(x^0)\right] \quad \text{(Eq 32)}$$

A and B atom chemical potentials are respectively defined as the first derivatives of the total free energy with respect to the number N_{A} and N_{B} of A and B atoms. This leads to the following expressions:

$$\mu_{\text{A}}(x) = G(x) - xG'(x)$$
$$\mu_{\text{B}}(x) = G(x) + (1-x)G'(x) \quad \text{(Eq 33)}$$

which check the property $(N_{\text{A}} + N_{\text{B}})G(x) = N_{\text{A}}\mu_{\text{A}} + N_{\text{B}}\mu_{\text{B}}$.

Incorporating these expressions in Eq 32:

$$\Delta G^{\text{nuc}}(x^0) = G(y^{\text{e}}) - G(x^0) - (y^{\text{e}} - x^0)G'(x^0) \quad \text{(Eq 34)}$$

This shows that the nucleation free energy corresponds to the difference, calculated in the point of abscissa y^{e}, between the free energy and the tangent in x^0, as illustrated in Fig. 1.

It should be stressed, however, that this construction does not correspond to the maximal nucleation driving force. If the stoichiometry of the precipitates is allowed to vary, the maximal nucleation driving force is obtained for a cluster composition y^0 corresponding to the point where the tangent to the free energy is parallel to the tangent in point of abscissa x^0 (Fig. 8). Such a deviation of the nucleating phase from its equilibrium may be important to consider. An example is the precipitation of carbonitride precipitates in steels (Ref 33). The following considers that the free energy well defining the nucleating phase is deep enough that the compositions y^{e} and y^0 can be assumed identical. This question of the precipitate composition is revisited in "Nonstoichiometric Clusters" of the "Kinetic Approach" section of this article, where a general framework to treat variations of the precipitate composition is presented.

To go further, one must consider a precise function for the free energy. The regular solid solution is a convenient energetic model that is representative of a binary alloy. In this model, the free energy per atom is:

$$G(x) = kT[x\ln(x) + (1-x)\ln(1-x)] + x(1-x)\omega \quad \text{(Eq 35)}$$

where ω is the interaction parameter. When this parameter is positive, the alloy tends to unmix at low temperature, and the corresponding phase diagram possesses a two-phase region. For temperatures lower than $\omega/2k$, the free energy indeed has two minima, and its variation with the composition is similar to the one sketched in Fig. 1. The nucleation free energy of a solid solution quenched in a metastable state, as given by this thermodynamic model, is:

$$\Delta G^{\text{nuc}}(x^0) = (1-y^{\text{e}})kT\ln\left(\frac{1-x^{\text{e}}}{1-x^0}\right) + y^{\text{e}}kT\ln\left(\frac{x^{\text{e}}}{x^0}\right) + \omega(x^0 - x^{\text{e}}) \quad \text{(Eq 36)}$$

A useful approximation of this expression is the dilute limit corresponding to a small solubility limit, $x^{\text{e}} \ll 1$, and a small nominal concentration, $x^0 \ll 1$. In that case, one can keep only the major contribution in the nucleation free energy, leading to:

$$\Delta G^{\text{nuc}}(x^0) = y^{\text{e}}kT\ln\left(\frac{x^{\text{e}}}{x^0}\right) \quad \text{(Eq 37)}$$

This generally gives a good approximation of the nucleation free energy at low temperature for not-too-high supersaturations. It then allows predicting the main consequences of a variation of the solid-solution nominal composition on the nucleation. This approximation of the nucleation free energy in the dilute limit can be easily generalized to a multicomponent alloy.

Other thermodynamic approaches can be used to obtain expressions of the nucleation free energy. It is possible, for instance, to describe interactions between atoms with an Ising model. Chemical potentials entering in Eq 4 can then be calculated with the help of current thermodynamic approximations, such as mean-field approximations and low- or high-temperature expansions (Ref 34). Using the simple Bragg-Williams mean-field approximation, one indeed recovers the expression (Eq 36) corresponding to the regular solid-solution model. An example of this approach, starting from an atomic model, is given in Ref 17 and 35 for a face-centered cubic solid solution leading to the nucleation of a stoichiometric compound with the $L1_2$ structure, such as aluminum-zirconium or aluminum-scandium alloys. On the other hand, it is possible to use an experimental thermodynamic database, such as the ones based on the Calphad approach (Ref 36, 37), to calculate the nucleation free energy.

Elastic Contribution. Usually, the precipitating phase has a different structure or molar volume from the parent phase. If the interface between both phases remains coherent, an elastic contribution must be taken into account in the formation free energy of the clusters (Eq 3). Similar to the "chemical" nucleation free energy, this elastic contribution varies linearly with the volume, V, of the cluster. Its sign is always positive because there is an extra energy cost to maintain coherency at the interface. One can illustrate this elastic contribution by considering the case of a precipitating phase having a slightly different equilibrium volume from the parent phase, as

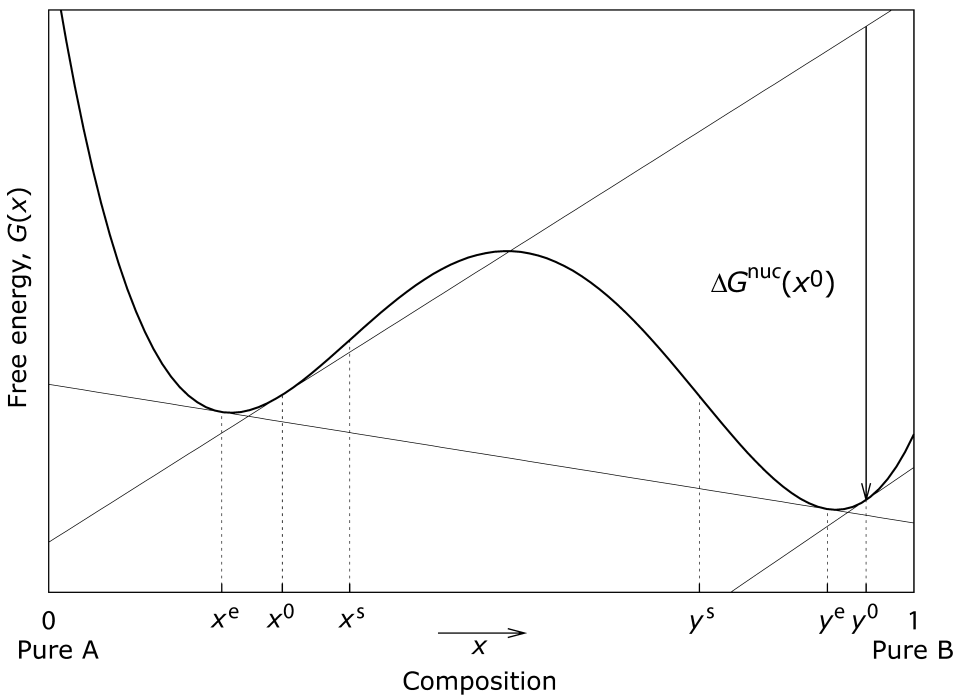

Fig. 8 Parallel tangent construction leading to the maximal nucleation driving force for precipitates having the composition y^0

well as different elastic constants. For the sake of simplicity, the assumption is that both phases have an isotropic elastic behavior characterized by their Lamé coefficients, λ and μ for the parent phase, and λ' and μ' for the precipitating phase. If a and $a(1 + \delta)$ are the respective lattice parameters of the two phases, the elastic energy necessary to embed a spherical cluster of volume V in an infinite elastic medium corresponding to the parent phase is:

$$\Delta G^{el} = V\frac{6\mu(3\lambda' + 2\mu')}{3\lambda' + 2\mu' + 4\mu}\delta^2 \qquad \text{(Eq 38)}$$

The model of the elastic inclusion and inhomogeneity developed by Eshelby (Ref 38–40) allows calculating the elastic energy in more complicated situations, when the inhomogeneity elastic behavior is anisotropic or when the inclusion stress-free strain is different from a simple pure dilatation. One can also deduce from this model the cluster shape minimizing its elastic self-energy. Nevertheless, this model is tractable only when the inclusion is an ellipsoid. When the elastic contribution becomes important compared to the interface one, the shape of the critical cluster strongly deviates from an ellipsoid. One can then use a diffuse interface phase-field model to determine the critical nucleus morphology and determine the associated nucleation activation energy (Ref 41, 42). However, in all cases, the extra energy cost arising from elasticity is positive and proportional to the inclusion volume. It thus reduces the absolute value of the nucleation driving force.

This inclusion model allows deriving the cluster self-elastic energy. However, the interaction of the cluster with the surrounding microstructure is ignored. In particular, one does not consider the elastic interaction between different clusters. Such an interaction is long range and cannot always be neglected. It may lead to self-organized morphological patterns due to preferred nucleation sites around already existing clusters. In the case where the strain induced by the microstructure varies slowly compared to the size of the nucleating cluster, it has been shown that the interaction elastic energy depends linearly on the cluster volume and is independent of its shape (Ref 43). This interaction energy, whose sign is not fixed, depends on the position of the cluster. It can be considered in the cluster formation free energy (Eq 3) to model strain-enhanced nucleation. Such a model is able to predict, for instance, variation of the nucleation driving force near an existing precipitate between the elastically soft and hard directions. A natural way to develop such a model is to use a phase-field approach (see the Appendix to this article).

Kinetic Approach

Predictions of the classical nucleation theory, that is, the steady-state nucleation rate and the incubation time, are approximated solutions of kinetic equations describing the time evolution of the system. Instead of using results of the classical nucleation theory, one can integrate these kinetic equations numerically. This kinetic approach is known as cluster dynamics. It rests on the description of the system undergoing phase separation as a gas of clusters that grows and decays by absorbing and emitting other clusters. In this section, the cluster gas thermodynamic formalism used by cluster dynamics is described first. Kinetic equations simulating the phase transformation are then presented. Finally, the link with classical nucleation theory is shown. It is generally assumed that the stoichiometry of the nucleating phase cannot vary. This is thus equivalent to considering the nucleation of clusters with a fixed composition that is known a priori. The end of this section shows how this strong assumption can be removed when one is interested in the nucleation of a multicomponent phase with a varying composition.

Cluster Gas Thermodynamics

The system is described as a gas of noninteracting clusters having a fixed stoichiometry corresponding to that of the precipitating phase at equilibrium with the parent phase. Clusters are groups of atoms that are linked by a neighborhood relation. If one wants to model precipitation in an unmixing alloy, for instance, one can consider that all solute atoms that are closer than a cutoff distance belong to the same cluster. No distinction is made between clusters belonging to the old or to the new phase. In this modeling approach, clusters are defined by a single parameter: their size or the number, n, of atoms they contain. The term G_n is the free energy of a cluster containing n atoms embedded in the solvent. G_n is a free energy and not simply an energy because of the configurational entropy; for a given cluster size, there can be different configurations having different energies. Thus, the associated partition function must be considered. If D_n^i is the number of configurations having the energy H_n^i for a cluster of size n, the cluster free energy is then defined as:

$$G_n = -kT\ln\left[\sum_i D_n^i \exp\left(-H_n^i/kT\right)\right] \qquad \text{(Eq 39)}$$

It is formally possible to divide this free energy into a volume and an interface contribution such as in the capillary approximation, except that the interface free energy, σ_n, may now depend on the cluster size. This free energy corresponds to an interface between the stoichiometric cluster and the pure solvent. Thus, in three dimensions:

$$G_n = ng^e + n^{2/3}(36\pi\Omega^2)^{1/3}\sigma_n \qquad \text{(Eq 40)}$$

where g^e is the free energy per atom of the bulk equilibrium precipitating phase, that is, without any interface. This is, by definition, the sum of the chemical potentials, μ_i^e, for each constituent of the cluster modulated by its atomic fraction, y_i^e:

$$g^e = \sum_i y_i^e \mu_i^e \qquad \text{(Eq 41)}$$

The interface free energy, σ_n, entering in Eq 40 is an average isotropic parameter, and clusters, on average, are therefore assumed to be spherical. One important difference with the capillary approximation is that this interface free energy now depends on the size n of the cluster. It is possible to compute the cluster free energy, G_n, starting from an energetic model describing interactions between atoms. For small clusters, one can directly enumerate the different configurations, i, accessible to a cluster of size n, and then directly build the free energy (Eq 39) (Ref 17, 32, 44). Because the degeneracy D_n^i grows very rapidly with the size of the cluster, this approach is limited to small clusters. For larger clusters, one can sample thermodynamic averages with Monte Carlo simulations to compute the free-energy difference between a cluster of size n and one of size $n + 1$ at a given temperature (Ref 44, 45). These simulations have shown that, in three dimensions, the size dependence of the interface free energy is well described for large enough clusters by a generalized capillary approximation:

$$\sigma_n = \sigma\left(1 + cn^{-1/3} + dn^{-2/3} + en^{-2/3}\ln(n)\right) \qquad \text{(Eq 42)}$$

where the temperature-dependent coefficients c, d and e correspond to the line, the point, and the undulation contributions to the interface free energy (Ref 45). They take into account the interface curvature. The asymptotic limit of Eq 42 corresponds to the constant interface free energy of the classic capillary approximation, which also depends on temperature.

Some other expressions have been proposed in the literature for the size dependence of the interface free energy. Gibbs (Ref 46) indeed obtained a differential equation of this size dependence. Integrating this expression, Tolman (Ref 47) obtained the following expression:

$$\sigma_n = \sigma\left[1 + \left(\frac{n_0}{n}\right)^{1/3}\right]^{-2} \qquad \text{(Eq 43)}$$

where n_0 is a parameter. One can see, however, that Eq 42 and 43 are equivalent up to the order $o(n^{-1/3})$ when n tends to infinity.

Consider an assembly composed of noninteracting clusters and model thermodynamics in the cluster gas approximation of Frenkel (Ref 48). If N_n is the number of clusters containing n atoms, the free energy of the system is given by:

$$G = G_0 + \sum_{n=1}^{\infty} N_n G_n - kT\ln(W) \qquad \text{(Eq 44)}$$

where G_0 is the free energy in the absence of clusters, and W is the number of different configurations accessible to the cluster assembly.

Assuming that each cluster, whatever its size, lies only on one site, and neglecting around each cluster all excluded sites that cannot be occupied by any other cluster, this number is simply given by:

$$W = \frac{N_0!}{\left(N_0 - \sum_{n=1}^{\infty} N_n\right)! \prod_{n=1}^{\infty} N_n!} \quad \text{(Eq 45)}$$

where N_0 is the number of sites accessible to the cluster. Application of the Stirling formula leads to the following estimation for the free energy:

$$G = G_0 + \sum_{n=1}^{\infty} N_n G_n + kT \sum_{n=1}^{\infty} N_n \ln(N_n) + kT\left(N_0 - \sum_{n=1}^{\infty} N_n\right) \ln\left(N_0 - \sum_{n=1}^{\infty} N_n\right) - N_0 \ln(N_0) \quad \text{(Eq 46)}$$

The equilibrium cluster size distribution can be deduced from this free energy. This distribution is obtained by minimizing Eq 46 under the constraint that the total number of atoms included in the clusters is fixed. Therefore, a Lagrange multiplier, μ, is introduced, and the grand canonical free energy is defined:

$$G - \mu \sum_{n=1}^{\infty} n N_n \quad \text{(Eq 47)}$$

The minimization of this grand canonical free energy with respect to the variables N_n leads to the equilibrium cluster size distribution that should check the equation:

$$\frac{N_n^{\text{eq}}}{N_0 - \sum_{n=1}^{\infty} N_n^{\text{eq}}} = \exp\left(-\frac{G_n - n\mu}{kT}\right) \quad \text{(Eq 48)}$$

The assumption of noninteracting clusters used to derive this equation is only valid in the dilute limit. It is therefore reasonable to neglect in Eq 48 the sum appearing in the rightside denominator compared to the number of accessible sites N_0. At equilibrium, the atomic fraction of clusters containing n atoms is then:

$$C_n^{\text{eq}} = \frac{N_n^{\text{eq}}}{N_s} = C_0 \exp\left(-\frac{G_n - n\mu}{kT}\right) \quad \text{(Eq 49)}$$

where $C_0 = N_0/N_s$, and N_s is the total number of sites. For homogeneous nucleation, all sites can act as nucleation centers: $N_0 = N_s$ and $C_0 = 1$. Sometimes, Eq 49 is written in its equivalent form:

$$C_n^{\text{eq}} = C_0 \left(\frac{C_1^{\text{eq}}}{C_0}\right)^n \exp\left(-\frac{G_n - nG_1}{kT}\right) \quad \text{(Eq 50)}$$

The quantities $G_n - n\mu$ and $G_n - nG_1$ should nevertheless not be confused; the first one is the cluster formation free energy in a cluster gas characterized by the parameter μ, whereas the last one is the energy difference between the cluster and the equivalent number of monomers. The following uses Eq 49 because it allows a direct link with the capillary approximation used by the classical nucleation theory.

It is interesting to understand the physical meaning of the Lagrange multiplier μ appearing in Eq 49. At equilibrium, the grand canonical free energy (Eq 47) is at a minimum. Then, for all sizes n:

$$\mu = \frac{1}{n}\frac{\partial G}{\partial N_n} \quad \text{(Eq 51)}$$

To calculate this derivative, the total number of atoms of type i is introduced:

$$M_i = y_i^e \sum_{n=1}^{\infty} n N_n \quad \text{(Eq 52)}$$

Equation 51 is equivalent to:

$$\mu = \frac{1}{n}\sum_i \frac{\partial G}{\partial M_i}\frac{\partial M_i}{\partial N_n} = \sum_i \mu_i^0 y_i^e \quad \text{(Eq 53)}$$

which uses the definition of the chemical potential—first derivative of the total free energy with respect to the number of atoms. Therefore, the Lagrange multiplier is nothing else than the chemical potentials of the different atomic species modulated by their atomic fraction. The fact that only one Lagrange multiplier is needed, and not one for each constituent, is a consequence of the initial assumption that the clusters have a fixed composition corresponding to the equilibrium one, y_i^e. Using the expression (Eq 40) of the cluster free energy and the definition (Eq 41) of the volume contribution, the equilibrium cluster size distribution given by the capillary approximation is recovered:

$$C_n^{\text{eq}} = C_0 \exp\left(-\frac{\Delta G_n}{kT}\right) \quad \text{(Eq 54)}$$

with:

$$\Delta G_n = n\Delta G^{\text{nuc}} + n^{2/3}\left(36\pi\Omega_1^2\right)^{1/3}\sigma_n \quad \text{(Eq 55)}$$

The nucleation free energy has the same expression as the one used in classical nucleation theory (Eq 4), but now the interface free energy depends on the cluster size.

It should be stressed that the cluster gas approximation is a thermodynamic model by itself; thermodynamic quantities such as chemical potentials are results and not input parameters of the model (Ref 49). This has important consequences for the kinetic approach of nucleation developed in the next section; in contrast with classical nucleation theory, one does not need to calculate the nucleation driving force to input it in the modeling.

One can use this cluster gas thermodynamic model to calculate the composition of the parent phase at the coexistence point between the parent and the nucleating phase, that is, the solubility limit. This coexistence point is defined by the equality of the chemical potentials μ_i^0 and μ_i^e. The nucleation free energy is thus null, and only the interface contributes to the cluster formation free energy (Eq 55). At the coexistence point, the composition of the parent phase is then:

$$x_i^e = y_i^e \sum_{n=1}^{\infty} n \exp\left(-\frac{n^{2/3}(36\pi\Omega_1)^2\sigma_n}{kT}\right) \quad \text{(Eq 56)}$$

The interface free energy fixes the solubility limit in the parent phase. This interface free energy is actually the key parameter of the nucleation kinetic approach. Even if its dependence on the cluster size is small, it is generally important to take it into account, because all thermodynamic quantities derive from it, and it enters in exponential terms such as in Eq 56.

Cluster Dynamics

For the sake of simplicity, in the following subsections homogeneous nucleation is considered. All monomers can be assumed equivalent; one does not need to distinguish between monomers lying on nucleation sites and free monomers.

Master Equation. Kinetics is described thanks to a master equation that gives the time evolution of the cluster size distribution. In many cases, one can assume that only monomers migrate. Therefore, this assumption is considered first and later the case where all clusters are mobile. When only monomers can migrate, the probability of observing a cluster containing n atoms obeys the differential equations:

$$\frac{\partial C_n}{\partial t} = J_{n-1\to n} - J_{n\to n+1} \quad \forall n \geq 2$$
$$\frac{\partial C_1}{\partial t} = -2J_{1\to 2} - \sum_{n\geq 2} J_{n\to n+1} \quad \text{(Eq 57)}$$

where $J_{n\to n+1}$ is the cluster flux from the class of size n to the class $n + 1$. This flux can be written:

$$J_{n\to n+1} = \beta_n C_n - \alpha_{n+1} C_{n+1} \quad \text{(Eq 58)}$$

where β_n is the probability per unit time for one monomer to impinge on a cluster of size n, and α_n is the probability for one monomer to leave a cluster of size n.

Condensation Rate. Expression of the condensation rate β_n can be obtained from physical considerations. This condensation rate must be proportional to the monomer concentration and can generally be written:

$$\beta_n = b_n C_1 \quad \text{(Eq 59)}$$

where b_n is an intrinsic property of the cluster of size n. In the ballistic regime, this factor is proportional to the surface of the cluster and to the jump frequency, Γ_1, of the monomer to impinge on the cluster. In the diffusion regime, this factor is proportional to the cluster radius and to the monomer diffusion coefficient, D_1. A general expression of the condensation rate, covering the ballistic and the diffusion regime,

has been proposed by Waite (Ref 24), who obtained:

$$\beta_n = 4\pi \frac{R_n^2}{R_n + \kappa} \frac{D_1}{\Omega_1} C_1 \quad \text{(Eq 60)}$$

where Ω_1 is the monomer volume, and R_n is the cluster capture radius. It can be assumed that this radius is close to the one corresponding to the more compact cluster shape, that is, a sphere, leading to:

$$R_n = \left(\frac{3n\Omega_1}{4\pi}\right)^{1/3} \quad \text{(Eq 61)}$$

The distance, κ, is given by the relation:

$$\kappa = \frac{D_1}{\lambda_1 \Gamma_1} \quad \text{(Eq 62)}$$

where λ_1 is the distance corresponding to the monomer last jump to become attached to the cluster. If $R_n \ll \kappa$, one recovers the expression of the condensation rate in the ballistic regime, and in the diffusive regime if $R_n \gg \kappa$. Equation 60 therefore shows that condensation on small clusters is generally controlled by ballistic reactions, and condensation on big clusters by diffusion.

The expressions used by classical nucleation theory for the condensation rate (Eq 12 and 13) are similar to the ballistic and diffusion limits of Eq 62. Nevertheless, a difference appears because the condensation rate of the classical nucleation theory is proportional to the solute concentration and not to the monomer concentration, as in Eq 62. It thus makes use of the total solute diffusion coefficient or jump frequency and not of the monomer diffusion coefficient or jump frequency. For a dilute system, one can consider that all the solute is contained in monomers. The condensation rates used by both approaches are then equivalent. However, the difference may be important for more concentrated systems. This point has been thoroughly discussed by Martin (Ref 49), who showed the equivalence in the dilute limit.

Evaporation Rate. By contrast with the condensation rate, the evaporation rate, α_n cannot generally be obtained directly. It has to be deduced from β_n using the equilibrium cluster size distribution (Eq 49). The evaporation rate is obtained assuming that it is an intrinsic property of the cluster and does not depend on the embedding system. Therefore, it is assumed that the cluster has enough time to explore all its configurations between the arrival and the departure of a monomer. This assumption is coherent with the fact that the clusters are only described through their sizes. Thus, α_n should not depend on the saturation of the embedding system. It could be obtained, in particular, by considering any undersaturated system. Such a system is stable, and there should be no energy dissipation. This involves all fluxes $J_{n \to n+1}$ equaling zero. Using Eq 58, the following is obtained:

$$\alpha_{n+1} = \bar{\alpha}_{n+1}(\mu) = \bar{\beta}_n(\mu) \frac{\bar{C}_n(\mu)}{\bar{C}_{n+1}(\mu)} \quad \text{(Eq 63)}$$

where overlined quantities are evaluated in the system at equilibrium characterized by its effective chemical potential, μ. In particular, the cluster size distribution is the equilibrium relation given by Eq 49. Using the expression (Eq 59) for the condensation rate, this finally leads to the following expression for the evaporation rate:

$$\alpha_{n+1} = b_n C_0 \exp[(G_{n+1} - G_n - G_1)/kT] \quad \text{(Eq 64)}$$

Because the condensation rate varies linearly with the monomer concentration, the contribution of the effective chemical potential cancels out in the expression (Eq 63) of α_n. The starting assumption is recovered; the evaporation rate depends only on the cluster free energy and not on the overall state of the cluster gas characterized by the effective chemical potential, μ. Using the generalized capillary approximation (Eq 55), one can show that the evaporation rate actually depends only on the cluster interface free energy:

$$\alpha_{n+1} = b_n C_0 \exp\Big\{ \left(36\pi {\Omega_1}^2\right)^{1/3} \times [(n+1)^{2/3}\sigma_{n+1} - n^{2/3}\sigma_n - \sigma_1]/kT \Big\} \quad \text{(Eq 65)}$$

The evaporation rate is then independent of the nucleation free energy, ΔG^{nuc}, which does not appear in any parameter. The nucleation free energy is implicit in cluster dynamics; there is no need to know it, but, if needed, one can calculate it from the cluster gas thermodynamic. This is in contrast with classical nucleation theory, where the nucleation free energy is an input parameter. On the other hand, cluster dynamics is very sensitive to the interface free energy as it appears in an exponential in the expression (Eq 65) of the evaporation rate. It is very important to have a correct evaluation of this interface free energy, especially of its variations with the cluster size, at least for small sizes.

In this approach, the evaporation rate is derived assuming that it is an intrinsic property of the cluster. Sometimes, one derives this parameter assuming instead that a hypothetical constrained equilibrium exists for the clusters in the supersaturated system; the equilibrium cluster size distribution (Eq 49) is taken to hold, although the system is supersaturated and cannot be at equilibrium. The evaporation rate is then obtained by imposing a detailed balance for Eq 58 with respect to this constrained equilibrium. Comparison with atomic simulation of the magnetization reversal of an Ising model (Ref 20) has shown that this constraint equilibrium assumption is good. The same conclusion was reached for subcritical clusters in the case of precipitation in the solid state (Ref 50). Katz and Wiedersich (Ref 51) pointed out that this constrained equilibrium assumption generally leads to the same expression of the evaporation rate as the intrinsic property assumption. In particular, this is true when the condensation rate varies linearly with the monomer concentration, as is the case here (Eq 59).

When the growth and decay of clusters is controlled by a reaction at the interface (ballistic regime), it is also possible to directly compute the condensation and evaporation rates (Ref 44). An atomistic model is used to describe the physical process at the atomic scale, and the corresponding rates are obtained by thermal averaging through Monte Carlo sampling. Detailed balance is now imposed at the atomic scale. This ensures that the detailed balance at the cluster scale, as given by Eq 63, is also checked. A huge computational effort is required, but this could be optimized by calculating the cluster interface free energies and their condensation and evaporation rates at the same time.

Numerical Scheme. The evolution of the cluster size distribution is obtained by integrating the set of equations (Eq 57). A direct approach can become cumbersome because the number of differential equations varies linearly with the size of the largest cluster. The maximum size of the cluster that can be considered is therefore limited by the number of differential equations that can be integrated. This problem can be circumvented by noticing that a detailed description is important only for small cluster sizes where quantities vary rapidly. For large sizes, variations are smoother, and an approximated description can be used. The easiest approach to do so is to consider that the size n is now a continuous variable. One can then develop Eq 57 and 58 to the second order about n, and the system evolution is described by the Fokker-Planck equation (Ref 52):

$$\frac{\partial C_n}{\partial t} = -\frac{\partial}{\partial n}[(\beta_n - \alpha_n)C_n] + \frac{1}{2}\frac{\partial^2}{\partial n^2}[(\beta_n + \alpha_n)C_n] \quad \text{(Eq 66)}$$

This continuous equation can be solved numerically by discretizing the continuous variable n. The best way to handle large cluster sizes is to use a varying increment greater than 1 and increasing with the cluster size. A convenient solution is an increment growing at a constant rate λ. The variable n is then discretized according to:

$$\begin{aligned} &n_j = j, \quad \forall j \le n_{\text{d}} \\ &n_j = n_{\text{d}} + \frac{1 - \lambda^{j - n_{\text{d}}}}{1 - \lambda}, \quad \forall j \ge n_{\text{d}} \end{aligned} \quad \text{(Eq 67)}$$

where n_{d} is the number of classes for which the discrete equation (Eq 57) is used. Above this size, one integrates instead the discretized version of Eq 66, which is:

$$\frac{\partial C_{n_j}}{\partial t} = \frac{1}{n_{j+1}-n_{j-1}}\left[\left(\beta_{n_j}-\alpha_{n_j}\right)+\frac{\beta_{n_j}+\alpha_{n_j}}{n_j-n_{j-1}} - \frac{\partial}{\partial n}\left(\beta_{n_j}+\alpha_{n_j}\right)\right]C_{n_{j-1}} + \left[-\frac{\beta_{n_j}+\alpha_{n_j}}{(n_{j+1}-n_j)(n_j-n_{j-1})} - \frac{\partial}{\partial n}\left(\beta_{n_j}-\alpha_{n_j}\right) - \frac{1}{2}\frac{\partial^2}{\partial n^2}\left(\beta_{n_j}+\alpha_{n_j}\right)\right]C_{n_j} + \frac{1}{n_{j+1}-n_{j-1}}\left[-\left(\beta_{n_j}-\alpha_{n_j}\right)+\frac{\beta_{n_j}+\alpha_{n_j}}{n_{j+1}-n_j} + \frac{\partial}{\partial n}\left(\beta_{n_j}+\alpha_{n_j}\right)\right]C_{n_{j+1}} \quad \text{(Eq 68)}$$

The evolution of the monomer concentration is approximated by:

$$\frac{\partial C_1}{\partial t} = -2\beta_1 C_1 + \alpha_2 C_2 + \sum_{j\geq 2}^{n_d}\left(\alpha_{n_j}-\beta_{n_j}\right)C_{n_j} + \sum_{j\geq n_d}\left(\alpha_{n_j}-\beta_{n_j}\right)\frac{n_{j+1}-n_{j-1}}{2}C_{n_j} \quad \text{(Eq 69)}$$

This numerical scheme is simple and allows large cluster sizes to be reached with a reasonable number of differential equations. Typically, it is possible to simulate clusters containing more than 4 million atoms by using 100 discrete classes and 400 continuous classes with a growing increment rate $\lambda = 1.03$. It should nevertheless be mentioned that this numerical scheme does not strictly conserve the matter. By using reasonable values for the discretization parameters λ and n_d, the losses are generally insignificant, but, in any case, they must be checked afterward to see if they are acceptable. One must also verify that the concentration of the largest size has not evolved at the end of the simulation.

Another numerical approach has been proposed by Kiritani (Ref 53) to solve the set of differential equations (Eq 57) while allowing large cluster sizes to be reached. His grouping method consists of replacing a group of master equations by only one equation representing the class. It assumes that the number of clusters of each size in a group is the same and that the condensation and evaporation rates for clusters in a group do not vary. Unfortunately, it has been shown that the result can be very bad if the grouping is not carried out properly (Ref 54). Furthermore, as in the previous scheme, it does not strictly conserve the matter, even with an optimized grouping. Golubov et al. (Ref 55) proposed a new grouping method that can conserve the matter. For this purpose, the first and second moments of each group are considered, and two equations for each class are obtained. The first moment equation controls the time evolution of the cluster size distribution, and the second moment equation ensures the matter conservation. Such a numerical scheme therefore requires twice as many equations as the one proposed previously.

The Link with Classical Nucleation Theory

The main results of classical nucleation theory have actually been derived from cluster dynamics, that is, from the master equation (Eq 57) describing the time evolution of the cluster population. This derivation is interesting because it allows a better understanding of the assumptions behind the classical nucleation theory. Moreover, it provides insights into how this theory can be further developed to broaden the range where it applies. In the following subsection, the definition of the critical size in cluster dynamics is compared with the classical ones, and then it is shown how the steady-state nucleation rate and the corresponding cluster size distribution can be derived from the master equation. The derivation of the incubation time is not given here but can be found in Ref 26 and 27, for instance.

Critical Size. Subcritical clusters are unstable; they have a higher probability to decay than to grow. On the contrary, supercritical clusters are stable and have a higher probability to grow than to decay. The critical size n^* is then defined as the size for which the condensation rate equals the evaporation rate:

$$\beta_{n^*} = \alpha_{n^*} \quad \text{(Eq 70)}$$

This definition is actually different from the one used by the classical nucleation theory, where the critical size is the size at which the cluster formation free energy is maximum. One can show that these two definitions are consistent and lead to the same expression in the limit of large cluster sizes. To do so, rewrite Eq 70 using the expressions of the condensation rate (Eq 59) and of the evaporation rate (Eq 64):

$$b_{n^*}C_1 = b_{n^*-1}C_0\exp\left(\frac{G_{n^*}-G_{n^*-1}-G_1}{kT}\right) \quad \text{(Eq 71)}$$

Then, assume that monomers are at local equilibrium; their concentration C_1 obeys the equilibrium cluster size distribution (Eq 49). One can thus eliminate in Eq 71 the monomer free energy G_1:

$$b_{n^*}\exp\left(\frac{\mu}{kT}\right) = b_{n^*-1}\exp\left(\frac{G_{n^*}-G_{n^*-1}}{kT}\right) \quad \text{(Eq 72)}$$

Using the definition $\Delta G_n = G_n - n\mu$ of the cluster formation free energy, Eq 72 can be rewritten:

$$\frac{b_{n^*-1}}{b_{n^*}}\exp\left(\frac{\Delta G_{n^*}-\Delta G_{n^*-1}}{kT}\right) = 1 \quad \text{(Eq 73)}$$

Using Eq 55 to express the cluster formation free energy, one finally obtains that the critical size verifies:

$$\frac{b_{n^*-1}}{b_{n^*}}\exp\left\{\frac{\Delta G^{\text{nuc}} + \left(36\pi\Omega_1^2\right)^{1/3}\times\left[n^{*2/3}\sigma_{n^*} - (n^*-1)^{2/3}\sigma_{n^*-1}\right]}{kT}\right\} = 1 \quad \text{(Eq 74)}$$

To go further, one needs to take the limit corresponding to large cluster sizes. One can then neglect the size dependence of the condensation rate prefactor, $b_{n^*-1} \sim b_{n^*}$, and of the cluster interface free energy, $\sigma_{n^*-1} \sim \sigma_{n^*} \sim \sigma$. At the critical size, one should therefore check:

$$\Delta G^{\text{nuc}} + \left(36\pi\Omega_1^2\right)^{1/3}\left[n^{*2/3} - (n^*-1)^{2/3}\right]\sigma = 0 \quad \text{(Eq 75)}$$

A limited expansion of Eq 75 for large sizes leads to the result:

$$n^* = \left[-\tfrac{2}{3}\frac{\left(36\pi\Omega_1^2\right)^{1/3}\sigma}{\Delta G^{\text{nuc}}}\right]^3 \quad \text{(Eq 76)}$$

One therefore recovers Eq 5 of the critical size with a geometric factor A corresponding to spherical clusters. The critical size considered by classical nucleation theory corresponds to the one of cluster dynamics in the limit of large cluster sizes. However, when the critical size is small, both definitions may differ. This coherence of both definitions at large size and this deviation at small sizes has been observed in atomic simulations (Ref 20).

The Steady-State Nucleation Rate. One can calculate the steady-state nucleation rate, J^{st}, corresponding to the master equation (Eq 57). To do so, one must make two assumptions:

- There is a small size below which clusters have their equilibrium concentration, given by Eq 49. Clusters smaller than the critical size appear and disappear spontaneously through thermal fluctuations, and their concentrations stay roughly at equilibrium. The smaller the cluster, the better this assumption. The most convenient choice is therefore to impose thermal equilibrium for monomers:

$$C_1(t) = C_1^{\text{eq}} = C_0\exp\left(-\frac{G_1-\mu(t)}{kT}\right) \quad \text{(Eq 77)}$$

- There is a maximum cluster size, N, above which the cluster concentration remains null: $C_N(t) = 0$. This assumption cannot be checked for a true steady state without invoking a demon that removes clusters that appear at the size N and dissolves them into monomers. Nevertheless, one can always define at a given time a size large enough so that the cluster distribution did not propagate to this size.

By definition, the steady-state nucleation rate can be calculated at any cluster size n. At the

steady-state, all cluster concentrations remain constant. As a consequence:

$$\frac{\partial J_{n\to n+1}}{\partial n} = 0 \qquad \text{(Eq 78)}$$

and the steady-state nucleation rate can be calculated at any given cluster size. Using the expression of the cluster flux (Eq 58) with Eqs 59 and 64 for the condensation and evaporation rates, one obtains:

$$J^{st} = b_n\left\{C_1C_n - C_{n+1}C_0\exp\left[\frac{G_{n+1}-G_n-G_1}{kT}\right]\right\},$$
$$n = b_nC_1\exp\left[-\frac{G_n-n\mu}{kT}\right]\left\{C_n\exp\left[\frac{G_n-n\mu}{kT}\right] - C_{n+1}\exp\left[\frac{G_{n+1}-(n+1)\mu}{kT}\right]\right\} \qquad \text{(Eq 79)}$$

This equation uses the fact that monomers are at equilibrium (Eq 77) to go from the first to the second line. After rearranging the terms between the left and right sides, a sum between a minimal and a maximal size is derived:

$$\sum_{n=n_1}^{n_2}\frac{J^{st}}{b_nC_1C_0\exp\left[-\frac{G_n-n\mu}{kT}\right]} = \frac{C_{n_1}}{C_0\exp\left[-\frac{G_{n_1}-n_1\mu}{kT}\right]} - \frac{C_{n_2+1}}{C_0\exp\left[-\frac{G_{n_2+1}-(n_2+1)\mu}{kT}\right]} \qquad \text{(Eq 80)}$$

$n_1 = 1$ is chosen so that the first term on the right side is equal to 1. With $n_2 = N - 1$, the second term is null; it is assumed $C_N = 0$, and the exponential is tending to ∞ for high enough N. This results in:

$$J^{st} = C_1C_0\frac{1}{\sum_{n=1}^{N-1}\frac{1}{b_n}\exp\left[\frac{G_n-n\mu}{kT}\right]} \qquad \text{(Eq 81)}$$

This gives an exact expression of the steady-state nucleation rate under both of the previous assumptions.

The sum appearing in Eq 81 can be easily evaluated. To do so, a continuous approximation is made to transform the sum into an integral. The cluster formation free energy, $\Delta G_n = G_n - n\mu$, presents a maximum at the critical size n^*. As a consequence, the main contribution to the integral arises from sizes around the critical size and can be evaluated by a Taylor expansion around n^*. Finally, neglecting the variations of b_n in front of the exponential leads to:

$$J^{st} = C_1C_0b_{n^*} \times \frac{1}{\int_1^{N-1}\exp\left[\left(\Delta G_{n^*} + \frac{1}{2}\frac{\partial^2\Delta G_n}{\partial n^2}\Big|_{n=n^*}(n-n^*)^2\right)\Big/kT\right]\mathrm{d}n} \qquad \text{(Eq 82)}$$

Changing the integration limits in $-\infty$ and $+\infty$, the result of classical nucleation theory is recovered:

$$J^{st} = \beta^*ZC_0\exp\left(-\frac{\Delta G^*}{kT}\right) \qquad \text{(Eq 83)}$$

where $\beta^* = C_1b_{n^*}$, $\Delta G^* = \Delta G_{n^*}$ and the Zeldovich factor is given by Eq 9.

The Steady-State Cluster Size Distribution. Once the steady-state nucleation rate is known, one can easily obtain the corresponding cluster size distribution. Equation 80 is again used with the limits $n_2 = N - 1$, so that the last term on the right side is still null, and with $n_1 = n$, the size for calculating the cluster concentration. This leads to the result:

$$C_n^{st} = C_0\exp\left[-\frac{G_n-n\mu}{kT}\right]\sum_{j=n}^{N}\frac{J^{st}}{b_nC_1C_0\exp\left[-\frac{G_j-j\mu}{kT}\right]} \qquad \text{(Eq 84)}$$

Similar to the steady-state nucleation rate, the sum can be evaluated by making a continuous approximation, developing the cluster formation free energy around the critical size, and considering the limit $N \to \infty$. One obtains:

$$C_n^{st} = C_0\exp\left[-\frac{G_n-n\mu}{kT}\right]\frac{J^{st}}{C_1C_0b_{n^*}} \int_n^{\infty}\exp\left[\left(\Delta G_{n^*} + \tfrac{1}{2}\,\frac{\partial^2\Delta G_j}{\partial j^2}(j-n^*)^2\right)\Big/kT\right]\mathrm{d}j = \tfrac{1}{2}\,\mathrm{erfc}[\sqrt{\pi}Z(n-n^*)]C_0\exp\left[-\frac{G_n-n\mu}{kT}\right] \qquad \text{(Eq 85)}$$

The stationary distribution therefore corresponds to the equilibrium one, reduced by a factor varying from 0 for large sizes to 1 for small sizes. Well below the critical size, that is, for $n \le n^* - \Delta n/2$ with Δn given by Eq 10, this factor differs only slightly from 1, and the stationary distribution corresponds to the equilibrium one. At the critical size n^*, this factor is exactly one-half, and in the vicinity of n^*, the stationary distribution can be approximated with Eq 8.

Discussion. This derivation of quantities predicted by classical nucleation theory from cluster dynamics formalism enlightens the approximations made by this theory. It assumes that the supersaturation is not too high, so that the critical size is large enough. This allows one to consider the size as a continuous instead of a discrete variable and to make a finite expansion of key parameters around the critical size. Classical nucleation theory may therefore appear as more restricted than the kinetic approach based on the master equation (Eq 57), but the situation is not so simple.

One severe restriction of cluster dynamics is the thermodynamic model on which it relies. It is based on the cluster gas model of Frenkel (Ref 48), which is valid for a dilute system. Strictly speaking, cluster dynamics should only be used in the dilute case. If one wants to study more concentrated systems, the cluster gas model must be extended. Such an extension has been performed by Lépinoux (Ref 56) and is presented in the section "Configurational Frustrations between Clusters" in this article. On the other hand, classical nucleation theory does not rely on the cluster gas thermodynamic model. Instead, it makes use of the nucleation driving force that may be calculated with any thermodynamic model, in particular, one better suited to concentrated systems. Therefore, it is not a problem to use the classical nucleation theory to study concentrated systems as long as one correctly calculates the nucleation driving force.

Both formalisms also differ in the way they describe the parent and the nucleating phases. In the classical theory, one differentiates both phases, and nucleation is described through hetero-phase fluctuations corresponding to precipitates embedded in the parent phase. Such a differentiation does not appear in the kinetic approach, where one deals with only one system that is described as a gas of clusters having a fixed stoichiometry and embedded in a pure solvent. This description difference may become relevant when modeling concentrated systems, because the values of the input parameters may then differ according to the chosen, thermodynamic or kinetic, approach. This is the case, for instance, of the interface free energy. In cluster dynamics, this corresponds to the energy cost of an interface between a cluster with a fixed stoichiometry and the pure solvent, whereas in classical nucleation theory, one should consider that the precipitate and the parent phase are not pure and that solubility exists in both phases. The concentration appearing in the expression of the condensation rate may also differ between both approaches, as already quoted in the previous section, "Condensation Rate," in this article. This is either the monomer concentration (cluster dynamics) or the total solute concentration (classical nucleation theory).

All these subtle differences between cluster dynamics and classical nucleation theory have been discussed by Martin (Ref 49) in the case of precipitation in the solid state. He showed that both approaches were consistent and led to the same expressions in the dilute limit.

Extensions of Cluster Dynamics

The master equation (Eq 57) can be modified to describe nucleation under less restricted conditions than the ones of the previous subsections and then to build extensions of the cluster dynamics. In particular, the assumptions that only monomers can react and that clusters have a fixed stoichiometry corresponding to the equilibrium nucleating phase can be removed.

Mobile Clusters. Until now, it was assumed that only monomers are mobile. This assumption is not always valid. There is no reason to think, for instance, that all clusters except monomers are immobile in solidification. Diffusion of small clusters can also happen in solid-solid phase transformations. An interesting example is copper precipitation in iron, where atomic simulations have revealed that clusters containing up to several tens of copper atoms can be much more mobile than individual copper atoms (Ref 57). The master equation should

therefore be modified to account for reactions involving clusters larger than monomers. Such a generalization of the cluster dynamics formalism has been performed by Binder and Stauffer (Ref 4–6).

The probability of observing a cluster containing n atoms now obeys the generalized master equation:

$$\frac{\partial C_n}{\partial t} = \tfrac{1}{2}\sum_{n'=1}^{n-1} J(n-n', n' \to n) - \sum_{n'=1}^{\infty} J(n, n' \to n+n') - J(n, n \to 2n) \quad \text{(Eq 86)}$$

where $J(n,n' \to n + n')$ is the cluster flux corresponding to the reaction between the classes n and n' to the class $n + n'$. The factor ½ appearing in Eq 86 accounts for overcounting the pairs $\{n - n',n'\}$ in the summation. In this equation, one should not forget that the reactions $n + n \rightleftharpoons 2n$ involve two clusters of size n. When reactions are limited to reactions involving monomers, n' can only take the value 1, and $n - 1$ in the first sum and 1 in the second sum; the classical master Eq 57 of cluster dynamics is recovered.

The cluster flux is the difference between the condensation of two clusters of sizes n and n' and the splitting of a cluster of size $n + n'$ into two clusters of sizes n and n':

$$J(n, n' \to n+n') = b(n, n' \to n+n')C_n C_{n'} - \alpha(n+n' \to n, n')C_{n+n'} \quad \text{(Eq 87)}$$

One then obtains an expression for the absorption coefficient $b(n, n')$. If the reaction is limited by the cluster diffusion, this coefficient is given by (Ref 24):

$$b(n, n' \to n+n') = 4\pi R_{n,n'}\frac{D_n + D_{n'}}{\Omega_1}, \quad \forall n \neq n'$$
$$b(n, n \to 2n) = 4\pi R_{n,n}\frac{D_n}{\Omega_1} \quad \text{(Eq 88)}$$

where $R_{n,n'}$ is a capture radius and can be approximated by the sum of the two reacting cluster radii. In the expression (Eq 13) used in the classical nucleation theory, this capture radius was identified with the radius of the critical cluster, and the monomer radius was neglected.

If the diffusion coefficients of the n-mers are not known, one can use an approximation proposed by Binder et al. (Ref 58, 59). They simply consider that cluster diffusion is due to jumps of atoms located at the interface. When an atom jumps over a distance r_s with a frequency Γ_s, the center of gravity of the cluster jumps over r_s/n. Since the number of possible jumps at the interface increases with its area as $n^{2/3}$, D_n depends on n as:

$$D_n = \Gamma_s\left(\frac{r_s}{n}\right)^2 n^{2/3} = D_1 n^{-4/3} \quad \text{(Eq 89)}$$

In the case of precipitation in the solid state, one should not forget that substitutional atoms diffuse through exchange with vacancies and that a vacancy enrichment at the cluster interface is possible. In such a case, Eq 89 must be corrected with a prefactor to consider the vacancy concentration at the interface (Ref 57). This vacancy segregation is the reason why clusters containing several copper atoms are more mobile than monomers in iron (Ref 57).

The evaporation rate is still obtained by assuming that it is an intrinsic property of the cluster (or imposing a constrained equilibrium), thus leading to:

$$\alpha(n+n' \to n, n') = b(n, n' \to n+n')C_0 \exp\left(\frac{G_{n+n'} - G_n - G_{n'}}{kT}\right) \quad \text{(Eq 90)}$$

All parameters are thus determined, and the master equation (Eq 86) can be numerically integrated.

Binder and Stauffer (Ref 4, 6) also extended classical nucleation theory to obtain expressions of the steady-state nucleation rate and the incubation time, taking into account the mobility of all clusters. They started from the master equation (Eq 86) and imposed the detailed balance corresponding to Eq 90. They obtained expressions similar to the classical ones—Eq 11 for the steady-state nucleation rate and Eq 14 for the incubation time—except that now the growing rate, β*, of the critical cluster incorporates contributions of all clusters. This growing rate is given by:

$$\beta^* = \sum_{n=1}^{n_c} b(n^*, n \to n+n^*)n^2 C_0 \exp\left(-\frac{G_n - n\mu}{kT}\right) \quad \text{(Eq 91)}$$

where n_c is a cut-off size corresponding to the correlation length of thermal fluctuations. It seems reasonable to identify this cut-off size with the critical size n*. When only reactions involving monomers can occur, the sum in Eq 91 is limited to the term $n = 1$, and one recovers the classical growing rate $\beta^* = b_{n^*}C_1^{eq}$. When reactions involving other clusters are possible, this growing rate increases. The mobility of small clusters therefore leads to an increase of the nucleation rate and a decrease of the incubation time by the same factor.

Nonstoichiometric Clusters. Until now, it has been assumed that clusters have a fixed stoichiometry corresponding to the equilibrium of the nucleating phase. In some systems, the composition of the nucleating phase can vary. One therefore must extend cluster dynamics to allow the cluster stoichiometry to vary (Ref 7).

To illustrate such an extension of the formalism, consider the example of a system where the nucleating phase is composed of two elements, A and B, and assume that the composition can vary. A cluster is then a group of A and B atoms that are linked by a neighborhood relation. If the clusters are homogeneous (no segregation of one element at the interface, for instance), they can simply be described by two variables: the number i and j of elements A and B they contain. Therefore, $G_{i,j}$ is the free energy of such a cluster. If the system is undersaturated, one can show that the concentration of $\{i,j\}$ clusters is given by the distribution:

$$C_{i,j}^{eq} = C_0 \exp -\left(-\frac{G_{i,j} - i\mu_A - j\mu_B}{kT}\right) \quad \text{(Eq 92)}$$

where μ_A and μ_B are Lagrange multipliers ensuring matter conservation for A and B and are related to their chemical potentials.

It is assumed that only monomers are mobile. The time evolution of clusters containing i A elements and j B elements is then governed by the master equation:

$$\frac{\partial C_{i,j}}{\partial t} = J_{i-1,j\to i,j} - J_{i,j\to i+1,j} + J_{i,j-1\to i,j} - J_{i,j\to i,j+1}, \quad \forall\{i,j\} \neq \{1,0\} \text{ and } \{i,j\} \neq \{0,1\}$$
$$\frac{\partial C_{1,0}}{\partial t} = -\sum_{i\geq 0}\sum_{j\geq 0} J_{i,j\to i+1,j} - J_{1,0\to 2,0}$$
$$\frac{\partial C_{0,1}}{\partial t} = -\sum_{i\geq 0}\sum_{j\geq 0} J_{i,j\to i,j+1} - J_{0,1\to 0,2} \quad \text{(Eq 93)}$$

Fluxes are written as a difference between the evaporation and the condensation of a monomer:

$$J_{i,j\to i+1,j} = b_{i,j\to i+1,j}C_{1,0}C_{i,j} - \alpha_{i+1,j\to i,j}C_{i+1,j}$$
$$J_{i,j\to i,j+1} = b_{i,j\to i,j+1}C_{0,1}C_{i,j} - \alpha_{i,j+1\to i,j}C_{i,j+1} \quad \text{(Eq 94)}$$

The condensation and evaporation rates are still linked by a detailed balance condition, leading to the relations:

$$\alpha_{i+1,j\to i,j} = b_{i,j\to i+1,j}\exp\left(\frac{G_{i+1,j} - G_{i,j} - G_{1,0}}{kT}\right)$$
$$\alpha_{i,j+1\to i,j} = b_{i,j\to i,j+1}\exp\left(\frac{G_{i,j+1} - G_{i,j} - G_{0,1}}{kT}\right) \quad \text{(Eq 95)}$$

One therefore needs a physical modeling of the condensation process to express the coefficients $b_{i,j\to i+1,j}$ and $b_{i,j\to i,j+1}$. The evaporation rates are then obtained by Eq 95, and the kinetics are obtained by integration of Eq 93.

Starting from the master equation (Eq 93), the classical nucleation theory has been extended to treat a multicomponent system. This was first performed by Reiss (Ref 7) for a binary system such as the one considered here and then extended by Hirschfelder (Ref 8) to a general multicomponent system. Both authors assumed that the growth of the critical nucleus was entirely driven by the free energy. It was realized later by Stauffer (Ref 9) that the growth direction in the $\{i,j\}$ plane may also be affected by the condensation coefficients, especially when coefficients corresponding to A and B condensation have very different values. He proposed an expression of the steady-state nucleation rate for the binary system that was then extended to a multicomponent system by

Trinkaus (Ref 10). All these approaches calculated the steady-state nucleation rate in the vicinity of the critical nucleus. Wu (Ref 11) instead defined a global nucleation rate that should correspond more closely to what can be measured experimentally. The following gives the expression of the steady-state nucleation rate for a binary system obeying the master equation (Eq 93) in the local approach as derived by Vehkamäki (Ref 12). Expressions in the more general case—multicomponent systems and mobile clusters other than monomers—can be found in the cited references.

The critical cluster corresponds to the saddle point of the cluster formation free energy $\Delta G_{i,j} = G_{i,j} - i\mu_A - j\mu_B$ appearing in the equilibrium distribution (Eq 92). It is thus defined by the equations:

$$\frac{\partial \Delta G_{i,j}}{\partial i} = 0 \quad \text{and} \quad \frac{\partial \Delta G_{i,j}}{\partial j} = 0 \tag{Eq 96}$$

ΔG^* is the corresponding formation free energy, and H^* is the Hessian matrix calculated for the critical cluster:

$$H^* = \begin{pmatrix} \left.\frac{\partial^2 \Delta G_{i,j}}{\partial i^2}\right|_{\{i,j\}^*} & \left.\frac{\partial^2 \Delta G_{i,j}}{\partial i \partial j}\right|_{\{i,j\}^*} \\ \left.\frac{\partial^2 \Delta G_{i,j}}{\partial i \partial j}\right|_{\{i,j\}^*} & \left.\frac{\partial^2 \Delta G_{i,j}}{\partial j^2}\right|_{\{i,j\}^*} \end{pmatrix} \tag{Eq 97}$$

This Hessian matrix has two eigenvalues. One of them is negative and gives the direction in the $\{i,j\}$ space corresponding to the maximal decrease of the critical cluster free energy. In the approach of Reiss and Hirschfelder, this direction corresponds to the nucleation flow. Nevertheless, one should generally take into account that the condensation rates for A and B elements may be different, because this will impact the direction of the nucleation flow. Therefore, a new matrix characterizing the condensation process for the critical cluster is defined:

$$\mathrm{B}^* = \left.\begin{pmatrix} C_{1,0} b_{i,j \to i+1,j} & 0 \\ 0 & C_{0,1} b_{i,j \to i,j+1} \end{pmatrix}\right|_{\{i,j\}^*} \tag{Eq 98}$$

The fact that this matrix is diagonal reflects the assumption that only reactions involving monomers are possible. The angle θ of the nucleation flow in the $\{i,j\}$ space is then defined by:

$$\tan\theta = \frac{-H^*_{11}\mathrm{B}^*_{11} + H^*_{22}\mathrm{B}^*_{22} - \sqrt{4H^{*2}_{12}\mathrm{B}^*_{11}\mathrm{B}^*_{22} + \left(H^*_{11}\mathrm{B}^*_{11} - H^*_{22}\mathrm{B}^*_{22}\right)^2}}{2H^*_{12}\mathrm{B}^*_{11}} \tag{Eq 99}$$

The equivalent of the Zeldovitch factor is given by:

$$Z = -\frac{H^*_{11} + 2H^*_{12}\tan\theta + H^*_{22}\tan^2\theta}{(1+\tan^2\theta)\sqrt{|\det(H^*)|}} \tag{Eq 100}$$

and the average growth rate of the critical cluster by:

$$\beta^* = \frac{\det(\mathrm{B}^*)}{\mathrm{B}^*_{11}\sin^2\theta + \mathrm{B}^*_{22}\cos^2\theta} \tag{Eq 101}$$

With these definitions, the steady-state nucleation rate keeps its usual expression:

$$J^{\mathrm{st}} = \beta^* Z C_0 \exp\left(-\frac{\Delta G^*}{kT}\right) \tag{Eq 102}$$

Configurational Frustrations between Clusters. Cluster dynamics simulations rely on the cluster gas approximation derived in the section "Cluster Gas Thermodynamics" in this article. This thermodynamic approximation, initially introduced by Frenkel (Ref 48), is strictly valid only in the dilute limit. It indeed assumes that the space occupied by the clusters can be neglected when computing the configurational partition function (Eq 45) of the cluster gas; each cluster occupies only one site, no matter its size. Lépinoux (Ref 56) has shown that this approximation can be improved to properly take into account frustrations between clusters, that is, the space forbidden to a given cluster by other clusters. This allows the modeling of systems that are not as dilute as required by Frenkel's treatment.

Note that $V_{j,n}$ is the number of sites that a cluster of size j forbids to a cluster of size n. According to Lépinoux (Ref 56), the equilibrium cluster size distribution is given by:

$$C_n^{\mathrm{eq}} = C_0 \exp\left(-\frac{G_n - n\mu}{kT}\right) \exp\left(-\sum_j C_j^{\mathrm{eq}} V_{j,n}\right) \tag{Eq 103}$$

or equivalently:

$$C_n^{\mathrm{eq}} = C_0 \left(\frac{C_1^{\mathrm{eq}}}{C_0}\right)^n \exp\left(-\frac{G_n - nG_1}{kT}\right) \exp\left[-\sum_j C_j^{\mathrm{eq}}\left(V_{j,n} - nV_{1,n}\right)\right] \tag{Eq 104}$$

It is clear that Frenkel's approximation corresponds to neglecting all exclusion volumes ($V_{j,n} = 0$). When exclusion volumes are considered, only an implicit expression of the size distribution is obtained; equilibrium cluster size concentrations, C_j^{eq}, are required to evaluate the right side of Eq 103 or 104. A self-consistent loop can be used to evaluate the equilibrium distribution, starting from the distribution given by Frenkel's approximation (Eq 49 or 50).

The exclusion volumes can be approximated by identifying a cluster of size n with a sphere of radius R_n. This leads to:

$$V_{j,n} = \frac{4\pi}{3}\left(R_j + R_n\right)^3 \tag{Eq 105}$$

The radii R_n depend on the temperature because a cluster becomes less compact with higher temperatures due to its configurational entropy. Nevertheless, it can be reasonably assumed that these radii are close to the ones corresponding to the more compact cluster shape (Ref 56), and Eq 61 can be used.

The second step is to obtain the kinetic coefficients α_n and β_n. As previously mentioned, the condensation rate β_n is obtained by the proper physical modeling of the condensation process, leading to an expression of the form in Eq 59. However, it is no longer possible to assume that the evaporation rate is an intrinsic property of the cluster; the obtained expression would violate the assumption because of the frustration contribution in the cluster size distribution. The constrained equilibrium is not satisfactory either, because it leads to a diverging frustration correction and hence diverging evaporation rates in supersaturated systems. There is actually no framework that allows rigorously deriving the evaporation rate from the condensation rate, taking into account cluster frustrations. It seems that the most reasonable scheme is to consider that the classical expression (Eq 64) of the evaporation rate must be corrected from frustrations caused by the instantaneous cluster size distribution and not by a hypothetical equilibrium one:

$$\alpha_{n+1}(t) = b_n C_0 \exp\left(\frac{G_{n+1} - G_n - G_1}{kT}\right) \exp\left[\sum_j C_j(t)\left(V_{j,n+1} - V_{j,n} - V_{j,1}\right)\right] \tag{Eq 106}$$

This set of condensation and evaporation rates ensures that the cluster distribution evolves toward the equilibrium distribution given by Eq 103 for subcritical clusters. Equation 106 clearly shows that the evaporation rate is no longer an intrinsic property of the cluster, because it now depends on the whole cluster distribution. Moreover, because this parameter depends on the instantaneous concentrations $C_j(t)$, it must be calculated at each time step. When the system is dilute, the frustration correction in Eq 106 becomes negligible, and the classical expression of the condensation rate is recovered. Comparisons with atomic simulations (Ref 50, 56) have shown that this treatment of cluster frustrations greatly improves the ability of cluster dynamics to describe nucleation kinetics for high supersaturations.

Limitations of the Cluster Description

The previous extensions of cluster dynamics have allowed the removal of two limitations of classical nucleation theories due to initial simplifying assumptions:

- Only monomers are mobile, and therefore, only reactions involving monomers are possible.
- The cluster stoichiometry is fixed and known a priori. It is assumed to correspond to the composition of the nucleating phase at equilibrium with the mother phase.

The extension to mobile clusters is quite straightforward, and that to nonstoichiometric clusters shows that it was possible to take into account a nonfixed cluster composition.

The composition of the nucleating cluster was found to be the one minimizing the work, ΔG^*, necessary to form them.

Nevertheless, some limitations still remain for this nucleation modeling approach. One of these limitations arises from the needed assumption that clusters are homogeneous. This assumption is induced by the fact that clusters are only described by the number of elements they contain. This is not always valid because segregation may occur in some systems; it can be more favorable for one element to lie at the interface between the cluster and the matrix instead of in the core of the cluster. In such a case, it is necessary to introduce at least one more parameter to describe the cluster structure. Binder and Stauffer (Ref 4) have extended cluster dynamics formalism to incorporate additional parameters describing cluster internal degrees of freedom, but the application of the formalism appears quite intricate.

Cahn and Hilliard (Ref 60) proposed a modeling approach different from the classical one presented here, which is based on a cluster description. Their approach agrees with the classical one at low supersaturations and underlines some limitations of the classical approach with increasing supersaturations. They showed that the work, ΔG^*, required to form a critical cluster becomes progressively less than that given by the classical theory and continuously approaches zero at the spinodal limit, thus for a finite supersaturation. By contrast, the classical theory predicts that this work becomes zero only for an infinite supersaturation (Eq 6). Moreover, the classical theory assumes that clusters are homogeneous and that their composition is the one minimizing the work, ΔG^*. Cahn and Hilliard showed that the composition at the center of the nucleus approaches that of the exterior mother phase when the supersaturation tends to the spinodal limit, and that the interface becomes more diffuse until eventually no part of the nucleus is even approximately homogeneous. The last disagreement found with the classical theory is the variation of the critical cluster size. They showed that this size first decreases, passes through a minimum, and then increases to become infinite when the supersaturation increases and approaches the spinodal limit. Nevertheless, some recent experiment observations (Ref 61, 62) have contradicted this last point, showing no divergence of the cluster critical size when approaching the spinodal limit.

Conclusions

Two different approaches based on an equivalent cluster description can therefore be used to model nucleation in a phase-separating system. In the classical nucleation theory, one obtains expressions of the nucleation rate and the incubation time. These expressions depend on a limited number of input parameters: the nucleation driving force, the interface free energy, and the condensation rate. On the other hand, the kinetic description of nucleation relies on a master equation. Cluster dynamics simulations, that is, the integration of this master equation, allow the time evolution of the cluster size distribution to be obtained. The input parameters needed by such simulations are the cluster condensation rates and the cluster free energies. At variance with classical nucleation theory, no external thermodynamic model is needed to calculate the nucleation driving force; cluster dynamics simulations possess their own thermodynamic model, the cluster gas. As shown previously, both approaches are intrinsically linked, but it is worth saying that they differ in the way they can be used to model the kinetics of phase transformations. Classical nucleation theory is able to model only the nucleation stage. To model the whole kinetics, one must couple this theory with classical descriptions of the growth and coarsening stage. Such a coupling can be done following the Wagner and Kampmann approach (Ref 63, 64). On the other hand, the cluster dynamics modeling approach is not restricted to the nucleation stage. It also predicts growth and coarsening kinetics. To conclude, this cluster approach is well suited when one knows what the nucleating new phase looks like. Such information is not always available a priori. One then must use other modeling techniques. These can be atomic simulations, such as molecular dynamics (Ref 65, 66), for condensation of a gas into a liquid or crystallisation of a liquid, or kinetic Monte Carlo (Ref 67–69) for solid-solid phase transformations, or phase-field simulations (see the Appendix at the end of this article). These simulations are computationally much more time-consuming and, as a consequence, are limited to the study of high enough supersaturations. Nevertheless, they can be very useful for understanding what happens in the nucleation stage and then building a classical model based on a cluster description and extending the range of supersaturations that can be simulated. Moreover, these atomic or phase-field simulations can be a convenient way to calculate the input parameters needed by classical theories.

Appendix—Phase-Field Simulations

The phase-field approach describes the different phases through continuous fields such as the atomic concentration or long-range-order parameters. The spatial and temporal evolution of the microstructure is then driven by differential equations obeyed by these fields. Because this technique is the object of the article "Phase-Field Modeling of Microstructure Evolution" in this Volume, this Appendix addresses how nucleation can be handled in such simulations.

The main advantage of phase-field simulations is that all spatial information on the microstructure is obtained. This is in contrast with classical approaches where a limited number of information is known, such as the flux of nucleating particles (classical nucleation theory) or the cluster size distribution (cluster dynamics). This may make the phase-field approach an attractive technique for modeling nucleation in specific situations. Indeed, such simulations perfectly take into account phase inhomogeneities. These inhomogeneities can be, for instance, a solute segregation in the vicinity of a defect such as a dislocation. Phase-field simulations therefore allow the description of heterogeneous nucleation associated with a variation of the driving force. Moreover, in the case of solid-solid phase transformations, the elastic energy is fully contained in the calculation of the system free energy (Ref 41). One therefore does not need a specific expression for the elastic self-energy of a nucleating particle nor for its elastic interaction with the existing microstructure. The correlated and collective nucleation due to elastic interaction between precipitates is naturally described. Two different roads have been proposed to include nucleation in phase-field simulations.

One can use the phase-field approach to calculate spatial variations of the concentrations and the order parameters describing the different phases as well as the inhomogeneous strain created by the microstructure. One then calculates the nucleation free energy as a function of the local phase fields and the local strain. Finally, the expression of the nucleation rate given by the classical theory is used to seed the phase-field simulations with new nuclei (Ref 70–72). In this way, one obtains a spatial variation of the nucleation rate caused by the microstructure inhomogeneities.

The phase-field approach offers another way to model nucleation without relying on the classical theory. One can add to the equations describing the phase-field evolution a stochastic term through a Langevin force to describe thermal fluctuations. This allows nucleation to proceed. Phase-field simulations can then naturally describe the spatial and temporal evolution of the microstructure, from the nucleation to the coarsening stage (Ref 73–75). Nevertheless, this description is usually only qualitative; to obtain a fully quantitative modeling, the amplitude of the Langevin force must be carefully set. In particular, it must depend on the coarse-graining size similar to the other ingredients of the simulation (chemical potentials, mobilities, stiffness coefficients) (Ref 76). Such phase-field simulations that naturally handle nucleation through thermal fluctuations suffer from the small time-step needed to catch the rare event of a nucleating particle. On the other hand, simulations using an explicit description of the nucleation do not have this drawback.

ACKNOWLEDGMENT

The author thanks Bernard Legrand, Georges Martin, Maylise Nastar, and Frédéric Soisson for fruitful discussions and their careful reading of the manuscript.

REFERENCES

1. M. Volmer and A. Weber, Keimbildung in Übersättigten Gebilden, *Z. Phys. Chem. (Leipzig)*, 119, 1926, p 277
2. L. Farkas, Keimbildungsgeschwindigkeit in Übersättigten Dämpfen, *Z. Phys. Chem. (Leipzig)*, 125, 1927, p 239
3. R. Becker and W. Döring, Kinetische Behandlung der Keimbildung in Übersättigten Dämpfen, *Ann. Phys. (Leipzig)*, 24, 1935, p 719
4. K. Binder and D. Stauffer, Statistical Theory of Nucleation, Condensation and Coagulation, *Adv. Phys.*, 25, 1976, p 343
5. K. Binder, Theory for the Dynamics of "Clusters." II. Critical Diffusion in Binary Systems and the Kinetics of Phase Separation, *Phys. Rev. B*, 15, 1977, p 4425
6. K. Binder, Theory of First-Order Phase Transitions, *Rep. Prog. Phys.*, 50, 1987, p 783
7. H. Reiss, The Kinetics of Phase Transitions in Binary Systems, *J. Chem. Phys.*, 18, 1950, p 840
8. J.O. Hirschfelder, Kinetics of Homogeneous Nucleation on Many-Component Systems, *J. Chem. Phys.*, 61, 1974, p 2690
9. D. Stauffer, Kinetic Theory of Two-Component ("Hetero-Molecular") Nucleation and Condensation, *J. Aerosol. Sci.*, 7, 1976, p 319
10. H. Trinkaus, Theory of the Nucleation of Multicomponent Precipitates, *Phys. Rev. B*, 27, 1983, p 7372
11. D.T. Wu, General Approach to Barrier Crossing in Multicomponent Nucleation, *J. Chem. Phys.*, 99, 1993, p 1990
12. H. Vehkamäki, *Classical Nucleation Theory in Multicomponent Systems*, Springer, Berlin, 2006
13. J.W. Cahn, Phase Separation by Spinodal Decomposition in Isotropic Systems, *J. Chem. Phys.*, **42,** 1965, p 93
14. K. Binder, Spinodal Decomposition, *Materials Science and Technology, A Comprehensive Treatment*, R.W. Cahn, P. Haasen, and E.J. Kramer, Ed., VCH, Weinheim, Vol. 5, 1991, pp. 405–471
15. G. Wulff, Zur Frage der Geschwindigkeit des Wachstums und der Auflösung der Kristallflächen, *Z. Kristallogr.*, 34, 1901, p 449
16. D.A. Porter and K.E. Easterling, *Phase Transformations in Metals and Alloys*, Chapman & Hall, London, 1992
17. E. Clouet, M. Nastar, and C. Sigli, Nucleation of Al_3Zr and Al_3Sc in Aluminum Alloys: From Kinetic Monte Carlo Simulations to Classical Theory, *Phys. Rev. B*, 69, 2004, p 064109
18. F. Soisson and G. Martin, Monte-Carlo Simulations of the Decomposition of Metastable Solid Solutions: Transient and Steady-State Nucleation Kinetics, *Phys. Rev. B*, 62, 2000, p 203
19. V.A. Shneidman, K.A. Jackson, and K.M. Beatty, Nucleation and Growth of a Stable Phase in an Ising-Type System, *Phys. Rev. B*, 59, 1999, p 3579
20. L. Maibaum, Phase Transformation near the Classical Limit of Stability, *Phys. Rev. Lett.*, 101, 2008, p 256102
21. D. Kashchiev, Solution of the Non-Steady State Problem in Nucleation Kinetics, *Surf. Sci.*, 14, 1969, p 209
22. D. Kashchiev, *Nucleation: Basic Theory with Applications*, Butterworth Heinemann, Oxford, 2000
23. G. Martin, The Theories of Unmixing Kinetics of Solid Solutions, *Solid State Phase Transformation in Metals and Alloys*, Les Éditions de Physique, Orsay, France, 1980, pp. 337–406
24. T.R. Waite, General Theory of Bimolecular Reaction Rates in Solids and Liquids, *J. Chem. Phys.*, 28, 1958, p 103
25. E. Clouet, A. Barbu, L. Laé, and G. Martin, Precipitation Kinetics of Al_3Zr and Al_3Sc in Aluminum Alloys Modeled with Cluster Dynamics, *Acta Mater.*, 53, 2005, p 2313
26. D.T. Wu, The Time Lag in Nucleation Theory, *J. Chem. Phys.*, 97, 1992, p 2644
27. V.A. Shneidman and M.C. Weinberg, Transient Nucleation Induction Time from the Birth-Death Equations, *J. Chem. Phys.*, 97, 1992, p 3629
28. K.F. Kelton, A.L. Greer, and C.V. Thompson, Transient Nucleation in Condensed Systems, *J. Chem. Phys.*, 79, 1983, p 6261
29. V.A. Shneidman and M.C. Weinberg, Induction Time in Transient Nucleation Theory, *J. Chem. Phys.*, 97, 1992, p 3621
30. J. Feder, K.C. Russell, J. Lothe, and G.M. Pound, Homogeneous Nucleation and Growth of Droplets in Vapours, *Adv. Phys.*, 15, 1966, p 111
31. D. Kashchiev, Nucleation at Existing Cluster Size Distributions, *Surf. Sci.*, 18, 1969, p 389
32. F. Berthier, B. Legrand, J. Creuze, and R. Tétot, Atomistic Investigation of the Kolmogorov-Johnson-Mehl-Avrami Law in Electrodeposition Process, *J. Electroanal. Chem.*, 561, 2004, p 37; Ag/Cu (001) Electrodeposition: Beyond the Classical Nucleation Theory, *J. Electroanal. Chem.*, 562, 2004, p 127
33. P. Maugis and M. Gouné, Kinetics of Vanadium Carbonitride Precipitation in Steel: A Computer Model, *Acta Mater.*, 53, 2005, p 3359
34. F. Ducastelle, *Order and Phase Stability in Alloys*, North-Holland, Amsterdam, 1991
35. E. Clouet and M. Nastar, Classical Nucleation Theory in Ordering Alloys Precipitating with $L1_2$ Structure, *Phys. Rev. B*, 75, 2007, p 132102
36. P. Spencer, A Brief History of CALPHAD, *Calphad*, 32, 2008, p 1
37. N. Saunders and A.P. Miodownik, *CALPHAD — Calculation of Phase Diagrams — A Comprehensive Guide*, Pergamon, Oxford, 1998
38. J.D. Eshelby, The Determination of the Elastic Field of an Ellipsoidal Inclusion, and Related Problems, *Proc. Roy. Soc. Lond. A*, 241, 1957, p 376
39. J.D. Eshelby, The Elastic Field Outside an Ellipsoidal Inclusion, *Proc. Roy. Soc. Lond. A*, 252, 1959, p 561
40. J.D. Eshelby, Elastic Inclusion and Inhomogeneities, *Progress in Solid Mechanics*, I.N. Sneddon and R. Hill, Ed., North Holland, Vol. 2, 1961, pp. 87–140
41. A.G. Khachaturyan, *Theory of Structural Transformations in Solids,* Wiley, New York, 1983
42. L. Zhang, L.-Q. Chen, and Q. Du, Morphology of Critical Nuclei in Solid-State Phase Transformations, *Phys. Rev. Lett.*, 98, 2007, p 265703
43. C. Shen, J.P. Simmons, and Y. Wang, Effect of Elastic Interaction on Nucleation: I. Calculation of the Strain Energy of Nucleus Formation in an Elastically Anisotropic Crystal of Arbitrary Microstructure, *Acta Mater.*, 54, 2006, p 5617
44. J. Lépinoux, Interfacial Reaction Rates and Free Energy of Cubic Clusters, *Philos. Mag.*, 85, 2005, p 3585
45. A. Perini, G. Jacucci, and G. Martin, Cluster Free Energy in the Simple-Cubic Ising Model, *Phys. Rev. B*, 29, 1984, p 2689; Interfacial Contribution to Cluster Free Energy, *Surf. Sci.*, 144, 1984, p 53
46. J.W. Gibbs, *Collected Works*, Vol. 1, *Thermodynamics*, Longmans-Green, New York, 1928
47. R.C. Tolman, The Effect of Droplet Size on Surface Tension, *J. Chem. Phys.*, 17, 1949, p 333
48. J. Frenkel, *Kinetic Theory of Liquids*, Dover Publications, New York, 1955
49. G. Martin, Reconciling the Classical Nucleation Theory and Atomic Scale Observations and Modeling, *Adv. Eng. Mater.*, 8, 2006, p 1231
50. J. Lépinoux, Modelling Precipitation in Binary Alloys by Cluster Dynamics, *Acta Mater.*, 57, 2009, p 1086
51. J.L. Katz and H. Wiedersich, Nucleation Theory without Maxwell Demons, *J. Colloid and Interface Science*, 61, 1977, p 351
52. N.M. Ghoniem and S. Sharafat, A Numerical Solution to the Fokker-Planck Equation Describing the Evolution of the Interstitial Loop Microstructure during Irradiation, *J. Nucl. Mater.*, 92, 1980, p 121
53. M. Kiritani, Analysis of the Clustering Process of Supersaturated Lattice Vacancies, *J. Phys. Soc. Jpn.*, 35, 1973, p 95
54. M. Koiwa, On the Validity of the Grouping Method —Comments on "Analysis of the Clustering Process of Supersaturated Lattice Vacancies," *J. Phys. Soc. Jpn.*, 37, 1974, p 1532
55. S.I. Golubov, A.M. Ovcharenko, A.V. Barashev, and B.N. Singh, Grouping Method for the Approximate Solution of a Kinetic Equation Describing the Evolution of Point-Defect Clusters, *Philos. Mag. A*, 81, 2001, p 643

56. J. Lépinoux, Contribution of Matrix Frustration to the Free Energy of Cluster Distributions in Binary Alloys, *Philos. Mag*., 86, 2006, p 5053
57. F. Soisson and C.-C. Fu, Cu-Precipitation Kinetics in α-Fe from Atomistic Simulations: Vacancy-Trapping Effects and Cu-Cluster Mobility, *Phys. Rev. B*, 76, 2007, p 214102
58. K. Binder and D. Stauffer, Theory for the Slowing Down of the Relaxation and Spinodal Decomposition of Binary Mixtures, *Phys. Rev. Lett*., 33, 1974, p 1006
59. K. Binder and M.H. Kalos, "Critical Clusters" in a Supersaturated Vapor: Theory and Monte Carlo Simulation, *J. Stat. Phys*., 22, 1980, p 363
60. J.W. Cahn and J.E. Hilliard, Free Energy of a Nonuniform System. III. Nucleation in a Two-Component Incompressible Fluid, *J. Chem. Phys*., 31, 1959, p 688
61. A. Pan, T. Rappl, D. Chandler, and N. Balsara, Neutron Scattering and Monte Carlo Determination of the Variation of the Critical Nucleus Size with Quench Depth, *J. Phys. Chem. B*, 110, 2006, p 3692
62. P.G. Debenedetti, Thermodynamics: When a Phase is Born, *Nature*, 441, 2006, p 168
63. R. Wagner and R. Kampmann, Homogeneous Second Phase Precipitation, *Materials Science and Technology, A Comprehensive Treatment*, R.W. Cahn, P. Haasen, and E.J. Kramer, Ed., Vol. 5, pp. 213–303, VCH, Weinheim, 1991
64. M. Perez, M. Dumont, and D. Acevedo-Reyes, Implementation of Classical Nucleation and Growth Theories for Precipitation, *Acta Mater*., 56, 2008, p 2119
65. M.P. Allen and D.J. Tildesley, *Computer Simulation of Liquids*, Clarendon Press, Oxford, 1987
66. D. Frenkel and B. Smit, *Understanding Molecular Simulation — From Algorithms to Applications*, Academic Press, San Diego, 2001
67. G. Martin and F. Soisson, Kinetic Monte Carlo Method to Model Diffusion Controlled Phase Transformations in the Solid State, *Handbook of Materials Modeling*, S. Yip, Ed., pp. 2223–2248, Springer, The Netherlands, 2005
68. P. Bellon, Kinetic Monte Carlo Simulations in Crystalline Alloys: Principles and Selected Applications, *Thermodynamics, Microstructure, and Plasticity*, A. Finel, D. Mazière, and M. Veron, Ed., pp. 395–409, Kluwer Academic, Dordrecht, 2002
69. F. Soisson, Applications of Monte Carlo Simulations to the Kinetics of Phase Transformations, *Thermodynamics, Microstructure, and Plasticity*, A. Finel, D. Mazière, and M. Veron, Ed., pp. 427–436, Kluwer Academic, Dordrecht, 2002
70. J.P. Simmons, C. Shen, and Y. Wang, Phase Field Modeling of Simultaneous Nucleation and Growth by Explicitly Incorporating Nucleation Events, *Scripta Mater*., 43, 2000, p 935
71. Y.H. Wen, J.P. Simmons, C. Shen, C. Woodward, and Y. Wang, Phase-Field Modeling of Bimodal Particle Size Distributions during Continuous Cooling, *Acta Mater*., 51, 2003, p 1123
72. C. Shen, J.P. Simmons, and Y. Wang, Effect of Elastic Interaction on Nucleation: II. Implementation of Strain Energy of Nucleus Formation in the Phase Field Method, *Acta Mater*., 55, 2007, p 1457
73. Y. Wang, H.-Y. Wang, L.-Q. Chen, and A.G. Khachaturyan, Microstructural Development of Coherent Tetragonal Precipitates in Magnesium-Partially-Stabilized Zirconia: A Computer Simulation, *J. Am. Ceram. Soc*., 78, 1995, p 657
74. Y. Le Bouar, A. Loiseau, and A.G. Khachaturyan, Origin of Chessboard-Like Structures in Decomposing Alloys. Theoretical Model and Computer Simulation, *Acta Mater*., 46, 1998, p 2777
75. Y.H. Wen, Y. Wang, and L.Q. Chen, Phase-Field Simulation of Domain Structure Evolution during a Coherent Hexagonal-to-Orthorhombic Transformation, *Philos. Mag. A*, 80, 2000, p 1967
76. Q. Bronchart, Y. Le Bouar, and A. Finel, New Coarse-Grained Derivation of a Phase Field Model for Precipitation, *Phys. Rev. Lett*., 100, 2008, p 015702

SELECTED REFERENCES

Focusing on nucleation

- F.F. Abraham, Homogeneous Nucleation Theory—The Pretransition Theory of Vapor Condensation, *Advances in Theoretical Chemistry,* H. Eyring and D. Henderson, Ed., Academic Press, New York, 1974
- K.F. Kelton, Crystal Nucleation in Liquids and Glasses, *Solid State Physics*, H. Ehrenreich and D. Turnbull, Ed., Academic Press, New York, Vol. 45, 1991, pp. 75–177
- K.C. Russell, Nucleation in Solids: The Induction and Steady State Effects, *Adv. Colloid Interface Sci*., 13, 1980, p 205
- D.T. Wu, Nucleation Theory, *Solid State Physics*, H. Ehrenreich and F. Spaepen, Ed., Academic Press, New York, Vol. 50, 1997, pp. 37–187

Phase transformations

- J.W. Christian, *The Theory of Transformations in Metals and Alloys—Part I: Equilibrium and General Kinetic Theory*, 2nd ed., Pergamon Press, Oxford, 1975
- A.G. Khachaturyan, *Theory of Structural Transformations in Solids*, Wiley, New York, 1983